


 Cite this: *Lab Chip*, 2026, 26, 1417

## A review of microfluidic technologies for thermal management in flexible electronics

 Mingzi Liu,<sup>†a</sup> Jiahao Sun,<sup>†b</sup> Zuowei Sun,<sup>†a</sup> Yawen Xiao,<sup>b</sup> Yi Chen,<sup>efg</sup>  
 Jiyu Li<sup>\*b</sup> and Xinge Yu<sup>id\*acd</sup>

Flexible electronics with the features of soft, ultrathin, and shape adaptable properties, are believed as next-generation devices for physiological monitoring, digital diagnostics, and human–computer interaction. With the development of devices towards miniaturization and integration, thermal management has emerged as an essential challenge, which not only influences device performance and long-term stability but also affects user comfort. Various thermal management strategies, including passive and active approaches, have been employed to regulate the operating temperature. Nevertheless, it is still challenging to develop thermal regulation systems with a large temperature regulation range, good temperature uniformity, and high mechanical flexibility. Recently, the microfluidics-based thermal regulation method has emerged as a promising method that integrates active and passive thermoregulation methods. This review explores the thermal management mechanisms enabled by microfluidic devices, emphasizing an integrated strategy that combines material selection, structural geometry, and system optimization to enhance thermal performance. We analyze heat transfer principles in microchannels and highlight applications in device-level thermal management, personal thermal regulation, and thermal regulation interface for human–machine interaction and healthcare, addressing their specific demands. Finally, we outline the challenges and future perspectives for advancing microfluidics-based thermal management systems, focusing on capability, integration, and applications.

 Received 23rd September 2025,  
 Accepted 26th November 2025

DOI: 10.1039/d5lc00906e

[rsc.li/loc](https://rsc.li/loc)

## 1. Introduction

### 1.1 Thermal challenges in flexible electronics

Flexible electronics, as an emerging technology, cover disciplines from materials science, to electrical engineering, to mechanical engineering, and to biomedical engineering, which expands the functionality and application scenarios of electronic devices.<sup>1</sup> Over the past decade, flexible electronics has emerged as a revolutionary technology, witnessing great advancements from the laboratory to practical implementations. By integrating functional components with

flexible substrates, flexible electronics can overcome the physical limitations of traditional rigid electronic devices and maintain stable performance under bending, twisting, or even stretching. In medical diagnostics, flexible bioelectronics are driving transformative advances in medical monitoring technology toward intelligent, miniaturized, and comfortable solutions.<sup>2</sup> These devices combine biosensors, data processing units, and wireless transmission modules to achieve precise acquisition and real-time analysis of physiological signals, including blood pressure,<sup>3</sup> heart rate,<sup>4</sup> and skin modulus.<sup>5</sup> Beyond biomedical applications, flexible electronics play a crucial role in the human–machine interface (HMI) and electronic skin (E-skin).<sup>6</sup> Through the high density of sensor array design and multifunctional integration, it significantly enhances the interactive capabilities of HMIs.<sup>7</sup> In the field of E-skin, flexible sensor arrays can simultaneously detect different physical parameters, including pressure<sup>8</sup> and temperature,<sup>9</sup> achieving sophisticated motion sensing and interactive functions. Particularly noteworthy are recent advancements in tactile feedback systems that integrate mechanical vibration,<sup>10</sup> electrical stimulation,<sup>11</sup> and heating units<sup>12</sup> to simulate texture, hardness, and temperature perception. These

<sup>a</sup> Department of Biomedical Engineering, City University of Hong Kong, Kowloon, Hong Kong, China. E-mail: xingeyu@cityu.edu.hk

<sup>b</sup> School of Biomedical Engineering, Shenzhen Campus of Sun Yat-sen University, Shenzhen, China. E-mail: lijy887@mail.sysu.edu.cn

<sup>c</sup> Institute of Digital Medicine, City University of Hong Kong, Kowloon, Hong Kong, China

<sup>d</sup> Hong Kong Center for Cerebro-Cardiovascular Health Engineering, Hong Kong Science Park, New Territories, New Territories, Hong Kong, China

<sup>e</sup> Department of Emergency Medicine, West China Hospital, Sichuan University/West China School of Nursing, Sichuan University, Chengdu, China

<sup>f</sup> Disaster Medical Center, Sichuan University, Chengdu, China

<sup>g</sup> Nursing Key Laboratory of Sichuan Province, Chengdu, China

<sup>†</sup> These authors contribute equally: Mingzi Liu, Jiahao Sun, Zuowei Sun.

developments have substantially improved immersion in virtual reality interactions and laid the technical foundation for next-generation AR/VR interfaces.<sup>13</sup>

Nowadays, flexible electronics have evolved into complex, multi-functional platforms and autonomous closed-loop systems, yet their increasing system complexity has led to substantial thermal challenges. With the widespread adoption of 5G technology, the power density of radio frequency (RF) modules and memory units in flexible electronics has risen sharply, making thermal management in high power-density electronics an increasingly critical issue. Artificial intelligence (AI) technology has also brought new challenges to the thermal management of flexible electronic devices.<sup>21</sup> With the significant increase in sensor density, there is an urgent need for AI and high-performance computing chips to process massive amounts of data. To minimize delays during wireless data transmission, the continuously generated data must be quickly processed and analyzed near the physical location of the sensors. For example, wearable medical monitoring sensors can acquire physiological indicators in real time, and intelligent analysis of large amounts of data can yield personalized health

patterns.<sup>22</sup> However, with the increasing demand for computing power, the excessive heat flux density in electronic products will lead to a sharp rise in temperature.<sup>23</sup> For instance, the peak heat flux density of a blade server central processing unit (CPU) ranges from 80 to 200 W cm<sup>-2</sup>, with localized heat flux reaching 1000 W cm<sup>-2</sup>.<sup>24</sup>

Excessive heat accumulation not only deteriorates long-term operational stability but also degrades signal quality. As wearable devices require direct skin contact, their operating temperature must be constrained within the human comfort range of 31.1–35.4 °C, imposing extremely demanding requirements on thermal management systems.<sup>25</sup> There are various factors limiting heat dissipation in flexible electronics. Among them, the intrinsic low thermal conductivity of polymer materials is a critical bottleneck. On the one hand, commonly used flexible substrates, such as polyimide (PI), polydimethylsiloxane (PDMS), and polyethylene terephthalate (PET), exhibit thermal conductivities ranging from 0.1 to 0.3 W m<sup>-1</sup> K<sup>-1</sup>,<sup>26</sup> which is two orders of magnitude lower than that of traditional rigid substrates *i.e.* silicon 150 W m<sup>-1</sup> K<sup>-1</sup>.<sup>27</sup> This severely impedes lateral heat diffusion, leading to localized heat accumulation



**Mingzi Liu**

*Mingzi Liu received his B.S. degree in Materials Engineering from Northwestern Polytechnical University, China, in 2021, and his M.S. degree in Electronic Science and Technology from Xi'an Jiaotong University, China, in 2024. He is currently pursuing his Ph.D. in Biomedical Engineering at City University of Hong Kong. His research interests focus on flexible wearable electronic devices and thermal management.*



**Jiahao Sun**

*Jiahao Sun received his B.S. degree in Biomedical Engineering from Sun Yat-sen University, China, in 2025. He is currently pursuing his M.S. degree in Biomedical Engineering at the same university. His current research focuses on radiative cooling and its applications in flexible biomedical systems.*



**Zuowei Sun**

*Zuowei Sun received the Ph.D. degree in information and communication engineering from Jilin University, Jilin, China, in 2024. He is now a postdoctoral fellow in Biomedical Engineering, City University of Hong Kong, China. His research interests include haptic interface, health monitoring systems, and human-machine interaction.*



**Yawen Xiao**

*Yawen Xiao is pursuing her Bachelor's degree in Biomedical Engineering at the School of Biomedical Engineering, Sun Yat-sen University, China. Her research interests include microfluidic systems and thermal management for biomedical applications.*

near the heat source. On the other hand, the low thermal conductivity of polymer substrates also induces severe phonon mismatch with functional layers, thereby creating significant interfacial thermal resistance that obstructs vertical heat transfer. More critically, the requirement for stretchability in certain flexible electronics poses substantial challenges to their thermal dissipation capabilities.<sup>28</sup> Stretchable circuit designs, such as well-established mechanical serpentine interconnects, impose greater thermal burdens compared to conventional layouts. These meandering traces are typically 3–5 times longer than straight-line pathways, proportionally increasing Joule heating under equivalent current conditions.<sup>29</sup> Consequently, optimizing thermal management in flexible electronics requires addressing material limitations and geometric constraints unique to deformable systems.

### 1.2 Advantages of microfluidics-based thermal management

Efficient thermal regulation in flexible electronic devices is essential for ensuring device durability and operational stability, while maintaining key features of integration, miniaturization, and conformability. A variety of thermal regulation approaches have been developed so far. Passive thermal management, utilizing natural heat transfer mechanisms, offers an energy-efficient and environmentally friendly approach for flexible electronics. The main categories of passive thermal regulation methods are summarized in Fig. 1. High thermal conductivity materials are crucial in these systems, enabling effective heat spreading from localized hotspots to larger dissipation areas. Thermal interface materials have been developed to bridge micro-scale gaps and accommodate surface irregularities to optimize thermal transport paths, thereby significantly improving heat conduction between heat sources and heat sinks.<sup>30</sup> Radiative cooling materials demonstrate zero power consumption

cooling by emitting mid-infrared radiation to outer space through the atmospheric high-transparency window (ATW).<sup>31,32</sup> Recent advancements achieve the integration of radiative cooling layers with flexible electronics.<sup>33,34</sup> However, radiative cooling systems exhibit significantly lower cooling power compared to active cooling methods, while demonstrating strong environmental dependence with a dramatic decline in performance under high humidity and windy conditions.<sup>35</sup> Another significant limitation is their inherently slow thermal response, typically requiring several minutes or even longer to reach thermal equilibrium. This delay prevents it from responding in real time to rapid changes in device heat generation, making it difficult to achieve dynamic and precise temperature control. Utilizing the high specific heat capacity through the phase change process to absorb or release heat, phase change materials (PCMs) can help maintain electronic devices within a safe temperature range. The phase change cooling mechanism has unique advantages in the thermal management of flexible electronics, including high heat dissipation power, ease of integration, and commonality.

Active thermal management refers to systems that achieve heat transfer through external input energy, relying mainly on mechanical components such as fans, micropumps, and compressors. As shown in Fig. 1, the most cutting-edge cooling technologies include thermoelectric,<sup>36</sup> electrocaloric,<sup>37</sup> and magnetocaloric methods.<sup>38</sup> Among them, thermoelectric materials stand out as a promising candidate for next-generation semiconductor cooling due to their strong temperature-changing capability and lack of moving parts. Electrocaloric and magnetocaloric technologies, despite being energy-efficient, still face material and engineering challenges that need to be addressed before widespread adoption.

Microfluidics is a multidisciplinary field focused on the control, separation, merging, and mixing of small volumes of



Jiyu Li

*Jiyu Li received his Ph.D. in Biomedical Engineering from City University of Hong Kong in 2021 and worked as a postdoctoral researcher with Prof. Xinge Yu until 2025. He is now a Research Fellow and Ph.D. supervisor at the School of Biomedical Engineering, Sun Yat-sen University, China. His current research focuses on flexible and wearable bioelectronics, soft materials, and personalized health monitoring systems.*



Xinge Yu

*Xinge Yu received his Ph.D. in Electronic Science and Technology from the University of Electronic Science and Technology of China and completed a joint Ph.D. program at Northwestern University, USA. He later worked as a postdoctoral researcher at the University of Illinois at Urbana-Champaign. He is currently a Professor in the Department of Biomedical Engineering and Associate Director of the Institute of Digital Medicine at City University of Hong Kong. His research focuses on skin-integrated and soft bioelectronics for health monitoring and human-machine interfaces.*

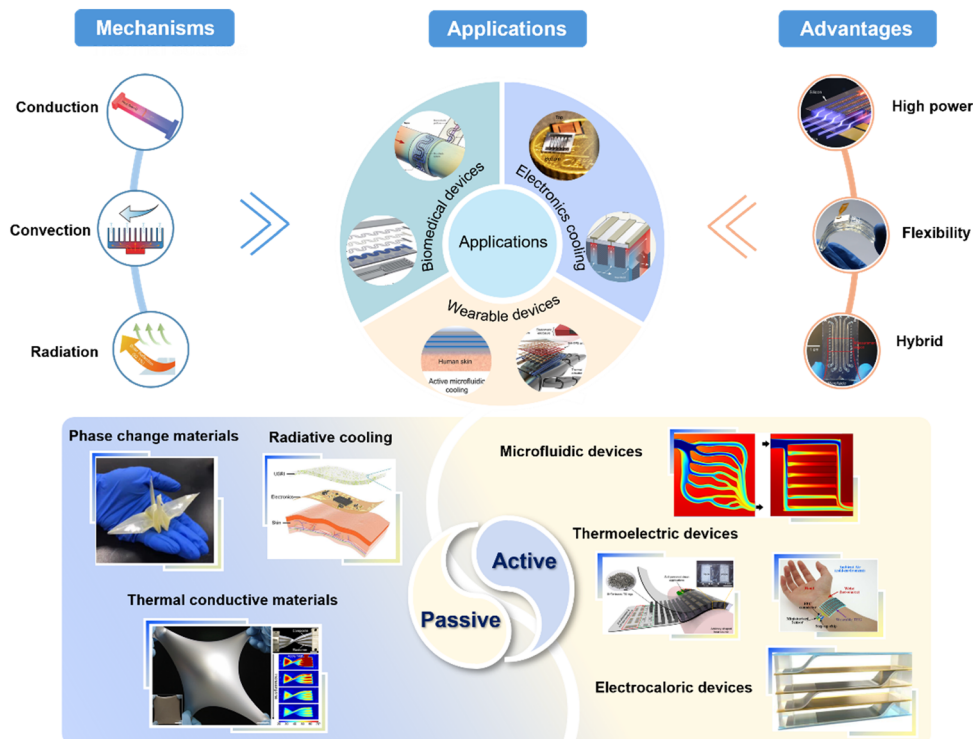


**Fig. 1** Summary of thermal management in flexible electronics, including heat transfer mechanisms, advantages and applications of microfluidics-based thermal management, and typical passive and active thermoregulation approaches (reproduced with permission from ref. 14, Copyright 2021, Elsevier; reproduced with permission from ref. 15, Copyright 2022, John Wiley and Sons; reproduced with permission from ref. 16, Copyright 2022, Springer Nature; reproduced with permission from ref. 17, Copyright 2022, the American Association for the Advancement of Science; reproduced with permission from ref. 18, Copyright 2020, Springer Nature; reproduced with permission from ref. 19, Copyright 2020, Springer Nature; reproduced with permission from ref. 20, Copyright 2020, Springer Nature).

liquid within microscale channels and structures.<sup>39</sup> The initial motivation of microfluidic technology aims to integrate all the functions of a biochemical laboratory into a single chip, evolving a new era of lab-on-chip (LOC) systems. Microfluidic devices have illustrated wide applications in biological reactions,<sup>40</sup> drug delivery,<sup>41</sup> and medical diagnostics,<sup>42</sup> as they can integrate liquid extraction, separation, and reaction into a single chip. As illustrated in Fig. 1, microchannel structures have demonstrated excellent heat dissipation capability for high power-density electronics while maintaining superior mechanical flexibility as a hybrid thermal regulation method.<sup>18,43</sup>

Soft lithography technology has greatly broadened the applications of microfluidics in flexible devices.<sup>44</sup> A variety of wearable devices have been proposed owing to the excellent mechanical properties of the matrix (PDMS,<sup>45</sup> paper,<sup>46</sup> and fabric<sup>47</sup>). By selecting substrate materials with different Young's moduli, both the upper and lower parts of the microchannels can maintain excellent flexibility. Thus, microfluidic cooling systems can be designed as compact, deformable structures that conform to flexible electronics. With their high-density microchannels and lightweight properties, these microfluidic devices are ideally suited for integration with flexible electronics while maintaining the overall system's profile and minimal weight. Unlike rigid

cooling solutions such as fins and fans, microchannels demonstrate superior adaptability for epidermal and stretchable applications, maintaining effective heat dissipation even under significant deformation.

Microfluidic systems offer a hybrid thermal management approach that combines the advantages of both passive and active cooling. When the thermal load of the system is low, these systems can dissipate heat through spontaneous fluid flow and natural heat transfer mechanisms. Meanwhile, high-surface-area conduction and phase-change cooling of fluid media promote heat transfer without external energy input. However, when localized heat flux becomes excessive, purely passive microchannel systems struggle to remove heat from hotspots effectively. In this situation, active cooling microfluidic systems that employ piezoelectric or electroosmotic pumps to enhance fluid circulation are capable of accelerating thermal transfer. To meet the demands of flexible circuit systems with transient, localized high-power operation, these systems integrate microvalves or micropumps that automatically adjust flow rates based on real-time temperature fluctuations of electronic components. This enables intelligent feedback-controlled cooling with on-demand power regulation. Under extreme thermal loads, such as during full CPU utilization, the system activates active pumping to boost cooling capacity rapidly. Conversely,

during periods of low thermal load, the passive heat absorption process of the fluid media maintains baseline cooling functionality, achieving energy-efficient heat dissipation.

In this review, we systematically discuss microfluidics-based systems for thermal management in flexible electronics. It begins with a fundamental discussion of the heat generation and transfer mechanisms, with particular emphasis on the unique thermal challenges of flexible electronics. We then critically analyze the latest advancements in both passive and active thermal regulation technologies, providing an assessment of their advantages and limitations. This review not only places much emphasis on the mechanism of microchannel-based thermal transfer, but also provides a comprehensive overview of channel materials and media materials, analyzing the effects of their mechanical and thermal properties. Furthermore, this review presents a structured discussion on applications, focusing on device-level thermal management for ensuring component reliability, personal thermal regulation aimed at human thermal comfort, and functional applications where thermal control enables novel capabilities. Through this comprehensive evaluation, we aim to provide valuable insights that will address current technical challenges and facilitate advancements in scientific research and industrial development.

## 2. Fundamentals of thermal management in flexible electronics

### 2.1 Heat generation and transfer mechanism

**2.1.1 Heat generation mechanism.** Recently, flexible electronic devices have advanced significantly toward higher integration and miniaturization. Following Moore's law, the feature size of transistors continues to shrink, significantly increasing the transistor density of chips. Recently, emerging technologies such as multi-core architectures and three-dimensional chip stacking have led to a remarkable enhancement in computational performance. Nevertheless, this trend has also introduced severe thermal challenges. Therefore, a deep understanding of heat generation mechanisms and effective thermal management strategies has become pivotal for advancing the further development and practical application of flexible electronics.

In electronic devices, Joule heating generated by current flowing through resistive components is the primary source of thermal energy. With the advancement of micro and nanofabrication technologies, such as photolithography, the dimensions of conductive traces in modern electronic components often reach micrometre scales, resulting in high current densities. A key fabrication technology for flexible electronics involves patterning stretchable electrode layers on polymer substrates using thin film metals and inorganic carbon materials. Techniques like E-beam evaporation and sputtering allow for the deposition of metal thin films on flexible substrates, with subsequent laser cutting or transfer

processes facilitating rapid electrode patterning. While serpentine geometries improve the electrode stretchability, they simultaneously increase the wiring density per unit area, exacerbating heat generation in electronic devices. For instance, a Kirigami-structured laser-induced graphene heater can reach over 40 °C in less than one minute at 36 V applied voltage.<sup>48</sup>

In addition to self-heating, flexible electronic devices inevitably experience thermal effects from solar radiation during operation, which may lead to electrical failures and performance degradation.<sup>25</sup> Consequently, environmental heat load is also a critical factor that must be considered in device thermal management. In outdoor applications, wearable devices with highly conductive materials can heat up rapidly under external heat or direct sunlight. This temperature rise not only compromises wearing comfort but also directly affects the signal quality of sensors. For example, skin-integrated photoplethysmography modules enable real-time pulse monitoring, but they are highly sensitive to temperature.<sup>33,49</sup> Prolonged sunlight exposure could decrease the output pulse signal quality and impair device functionality. In severe cases, key characteristic peaks may disappear, significantly reducing the reliability of physiological signals.

**2.1.2 Heat transfer mechanisms.** Thermal management, which aims to maintain the operational temperature of electronic devices within a reliable range by controlling heat flow, is particularly important in the design of highly integrated flexible electronics. The fundamental basis of thermal management is rooted in the manipulation of three classic heat transfer mechanisms: conduction, convection, and radiation. In wearable devices, thermal conduction often occurs between heat sources and the skin. This process involves heat transfer through lattice vibrations and the movement of free electrons. Metals exhibit high thermal conductivity because free electrons dominate heat transfer. In contrast, non-metallic materials like polymers and ceramics primarily rely on phonons, resulting in significantly lower thermal conductivity. The macroscopic behaviour of heat conduction follows Fourier's law:<sup>50</sup>

$$Q = -kA \frac{dT}{dx} \quad (1)$$

where  $Q$  represents the heat flow,  $k$  is the inherent thermal conductivity of materials,  $A$  is the cross-section area, and  $dT/dx$ , which is defined as the temperature gradient, describes how temperature varies with position. The negative sign here indicates the heat flow direction from the high to low temperature region. High thermal conductivity thermal interface materials have been widely employed. These materials facilitate effective heat transfer by constructing a 3D thermal conductive network, which minimizes interfacial gaps and reduces contact thermal resistance. This network efficiently enhances heat conduction from the heat source to the heat sink. Recent studies have shown that liquid metal-elastomer composites can achieve both high thermal

conductivity and mechanical stretchability, making them particularly suitable for flexible electronics.<sup>51</sup>

Heat convection involves thermal energy transfer through fluid motion, offering a mechanism to overcome the limited thermal conductivity of flexible substrates while improving cooling efficiency. Heat convection can be divided into natural convection and forced convection. Natural convection arises from temperature-induced density differences in fluids, such as the air convection around heat sinks. However, the convective heat transfer coefficient for air cooling is only 10–100 W m<sup>-2</sup> K<sup>-1</sup>, which requires a large temperature difference to achieve desirable heat flux.<sup>52</sup> Forced convection, on the other hand, involves mechanical means to drive fluid motion, such as fans or pumps generating convective flow to transfer heat. While heat fins can significantly improve convective cooling by increasing the surface area, their implementation in flexible wearable electronics remains challenging due to bulkiness and rigidity constraints. Similarly, conventional air-cooling methods, despite their rapid response and effective heat dissipation,

struggle to meet the flexibility and miniaturization requirements for wearable applications. Consequently, microchannel-based thermal management, which operates on the principle of heat convection, has become a promising thermal management approach due to its silent operation and ease of integration. The cooling power of convective heat transfer can be described as:<sup>63</sup>

$$P_{\text{cooling}} = hA\Delta T \quad (2)$$

where  $h$  is the convective heat transfer coefficient,  $A$  is the effective heat exchange area, and  $\Delta T$  is the temperature difference between the surface and fluid.

Thermal radiation describes the process in which an object excites its internal atoms, emitting electromagnetic waves to the surroundings. According to thermodynamic principles, all objects at temperatures above absolute zero spontaneously emit thermal radiation, facilitating heat transfer from higher-temperature objects to lower-temperature ones without any external energy input. The



**Fig. 2** Thermal management methods in flexible electronics. (A) Schematic of passive cooling strategies<sup>66</sup> (reproduced with permission from ref. 66, Copyright 2023, Elsevier); (B) ultrathin, soft, radiative cooling interfaces for advanced thermal management in skin electronics<sup>49</sup> (reproduced with permission from ref. 49, Copyright 2023, Elsevier); (C) schematic diagrams of the Seebeck effect (left) and Peltier effect (right) in thermoelectric materials<sup>73</sup> (reproduced with permission from ref. 73, Copyright 2024, John Wiley and Sons); (D) personal thermoelectric thermal regulation devices.<sup>75</sup> Diagrams of a thermoregulation vest and band with wearable TE (left). Structure of wearable TE devices with TE pillars, flexible electrodes, and stretchable sheets (right) (reproduced with permission from ref. 75, Copyright 2019, the American Association for the Advancement of Science). (E) Working mechanism of an EC thermal pump.<sup>37,78</sup> On the bottom left is the scheme of the thermodynamic cycle. On the bottom middle is the schematic illustration of the P(VDF-TrFE-CFE) heat pump under an electric field. On the bottom right is the schematic illustration of the EC heat pump after removing the electric field (reproduced with permission from ref. 37, Copyright 2017, Elsevier; reproduced with permission from ref. 78, Copyright 2021, the American Association for the Advancement of Science).

relationship between thermal radiation and an object's temperature is described as follows:<sup>64</sup>

$$P_{\text{rad}} = \varepsilon\sigma AT^4 \quad (3)$$

where  $\varepsilon$  denotes the emissivity of the material,  $\sigma$  is the Stefan–Boltzmann constant,  $A$  is the effective radiative area, and  $T$  represents the surface temperature of the object. Recently, radiative cooling materials have earned significant attention due to their environmental friendliness, zero energy consumption, and comfortable cooling effect.<sup>65</sup> The fundamental principle of radiative cooling is to dissipate heat into outer space *via* ATW.

## 2.2 Thermal management methods in flexible electronics

**2.2.1 Passive thermal management.** Passive cooling refers to heat management strategies that operate without external energy input, relying on intrinsic material properties and device structure to reject heat through thermal radiation, solar reflection, natural convection, and thermal conduction (Fig. 2A).<sup>66</sup> In flexible electronics, the thermal balance in flexible electronics is governed by four key heat flux components: radiative heat loss to the sky, absorbed solar radiation, convective/conductive heat exchange with the atmosphere, and internal heat generation from both electronics and the human body. In this section, we primarily introduce PCMs and radiative cooling materials due to their superior integration compatibility with flexible devices and effective thermal regulation performance.

PCMs act as a power-free heat sink by absorbing or releasing latent heat at a quasi-constant temperature during solid–liquid transition. In microfluidic systems for wearable applications, paraffins, fatty acids, and hydrated salts are common choices with tunable phase points in the range of 20–45 °C that match skin comfort.<sup>67</sup> To prevent leakage and enhance cycling durability, PCMs are typically microencapsulated in polymer shells or anchored within porous hosts (*e.g.*, silica, melamine-formaldehyde, cellulose aerogels). Microcapsules with narrow size distributions improve packing, lower percolation thresholds for heat flow modifiers, and mitigate volume-change stress over thousands of cycles. Beyond the fundamental issue of low thermal conductivity, the practical integration of PCMs into flexible electronics faces challenges in mechanical and thermal reliability. Firstly, the microencapsulation shell or porous support structure must withstand repeated bending or stretching without fracture, which would cause PCM leakage. Moreover, ensuring efficient heat transfer from the hot spot to the PCM domain under dynamic deformation is another key consideration for practical implementation.

Radiative cooling utilizes outer space as a heat sink by emitting thermal radiation through the ATW, achieving passive cooling without energy consumption.<sup>68,69</sup> For daytime applications, materials must minimize solar absorption to maintain net cooling power under sunlight. This can be

realized using polymer composites with micro- or nano-scale scatterers that induce strong Mie scattering across the solar spectrum while preserving high mid-infrared emissivity. Introducing high-index particles, hollow microspheres, or multilayer stacks increases backscattering and reduces parasitic heating.<sup>70</sup> For instance, Li *et al.*<sup>49</sup> fabricated an ultrathin, soft radiative-cooling interface by incorporating silica particles into a polymer for integration with skin electronics (Fig. 2B). This design maintained a solar reflectance of 91% and mid-infrared emissivity of 97%, demonstrating great potential in skin-integrated electronics. However, several challenges exist when implementing radiative cooling in flexible electronics. The limited heat flux capacity of radiative cooling also poses a challenge for applications with high power density, where additional active cooling methods may be required. In addition, environmental factors such as humidity, cloud cover, and atmospheric pollution can significantly reduce cooling performance. Zhang *et al.*<sup>71</sup> employed PTFE and pore engineering to fabricate a self-cleaning nanofiber membrane with a reflectance of 95.4% and emissivity of 95.8% for long-term daytime passive radiative cooling, showing significant application potential in clothing and buildings.

**2.2.2 Active thermal management.** Active thermal management technology enables high-precision temperature control through external energy input and dynamic regulation. Compared to passive thermal management, this approach offers advantages such as rapid response, controllability, and high heat dissipation efficiency, making it a critical solution for addressing thermal challenges in high power-density devices. In active cooling technologies, heat can be directionally transported through physical field regulation (*e.g.*, electric or magnetic fields) or transferred *via* mechanically driven methods like vapor-compression refrigeration, thereby achieving more efficient and controllable thermal management.<sup>72</sup> This section categorizes active thermal management strategies for flexible and wearable electronics. To provide a comprehensive comparison, the typical materials, thermoregulation performance, merits, and limitations of both passive and active thermoregulation methods are summarized in Table 1.

The thermoelectric (TE) effect, employing the Seebeck and Peltier effects, has emerged as a promising solid-cooling method. As shown in Fig. 2C, a typical thermoelectric module consists of a pair of thermoelectric elements (p-type and n-type semiconductors) connected in series with metal interconnects.<sup>57,73</sup> Charge carrier movement creates a temperature gradient for heating or cooling, reversible by switching current direction. Thermoelectric devices offer key advantages such as compact size, silent operation, and no moving parts, making them suitable for flexible electronics applications.<sup>74</sup> To achieve both a broad temperature regulation range and mechanical stretchability, Hong *et al.*<sup>75</sup> developed a novel approach for employing thermoelectric elements in personalized thermoregulation systems. As shown in Fig. 2D, they designed a sandwich structure

**Table 1** A summary of thermal management for flexible electronics

| Technique              | Representative material                                       | Thermoregulation performance   | Merits   | Limitations   | Ref. |
|------------------------|---|--|--|---|------|
| Conduction             | BN/PVA  | Thermal conductivity of $0.078 \text{ W m}^{-1} \text{ K}^{-1}$                                | Simple and low cost  | Failure under large thermal flow                                  | 53   |
|                        | SiC-epoxy   | $10.27 \text{ W m}^{-1} \text{ K}^{-1}$  | Flexible and compressive   | Mechanical failure under deformation                              | 54   |
| Radiative cooling      | Polystyrene-acrylic/TiO <sub>2</sub> /hollow SiO <sub>2</sub> | Temperature reduction $56 \text{ }^\circ\text{C}$ in electronics                               | Zero energy consumption  | Dependent on the atmospheric window                               | 49   |
|                        | PDMS nanofibers   | Temperature reduction $13.34 \text{ }^\circ\text{C}$ under xenon light irradiation             | Intrinsically flexible   | Limited cooling power   | 34   |
|                        | PMMA-SEBS   | Sub-ambient cooling of $6 \text{ }^\circ\text{C}$  | Achieve sub-ambient cooling  | Susceptible to weather and environmental conditions               | 33   |
| Phase change materials | <i>n</i> -Eicosane/melamine formaldehyde                      | Reduce peak skin temperature by 82%  | Cost-effective   | Limited cooling duration  | 55   |
|                        | Paraffin@copper/SE  | $18.6 \text{ }^\circ\text{C}$ lower than pure SE   | High energy storage density  | Requires regeneration and recharging period<br>Slow heat transfer | 56   |
| Thermoelectric         | Bi <sub>2</sub> Te <sub>3</sub>                               | $8.2 \text{ }^\circ\text{C}$ sub-ambient skin cooling  | Solid-state, no moving part  | Low energy conversion efficiency                                  | 57   |
|                        | Bi <sub>2</sub> Te <sub>3</sub>                               | A temperature rise of $20 \text{ }^\circ\text{C}$ and a decrease of $8 \text{ }^\circ\text{C}$ | Compact size<br>Precise and reversible operation (heating/cooling)           | Challenging thermal interface<br>High power demand                | 58   |
| Electrocaloric         | P(VDF-TrFE-CFE)   | Bidirectional thermoregulatory $2.9 \text{ K}$   | High thermodynamic efficiency  | High voltage  | 59   |
|                        | P(VDF-TrFE-CFE)   | Cooling $8.8 \text{ K}$ below ambient temperature  | Fast thermal response<br>Ultra-thin and lightweight                          | Limited cycle life<br>Small temperature span<br>High cost         | 60   |
| Microfluidics          | Poly(octanediolcitrate)-N <sub>2</sub> -perfluoropentane      | Cooling to $-20 \text{ }^\circ\text{C}$ in ambient temperature                                 | Effective heat dissipation for high power                                    | Dependent on pump   | 61   |
|                        | PDMS-water  | Temperature reduction $15 \text{ }^\circ\text{C}$ on the skin                                  | Stretchable channels design<br>Hybrid cooling mode<br>Intrinsically flexible | Potential leakage risk<br>High complexity                         | 62   |

comprising inorganic thermoelectric pillars embedded between two elastomer layers, which simultaneously minimizes heat leakage and maintains flexibility. This optimized design enables the device to achieve significant cooling performance, reaching a temperature differential of  $10 \text{ }^\circ\text{C}$  on the skin surface without requiring heat sinks. Despite their benefits, thermoelectric cooling systems are hindered by low energy conversion efficiency and challenging heat dissipation issues. Future research should prioritize implementing thermal interface materials, which can effectively minimize interfacial thermal resistance between thermoelectric materials and heat sinks and enhance thermal conductivity.

The electrocaloric (EC) effect provides a solid-state mechanism for cooling and heating through external electric field modulation.<sup>76,77</sup> Under an adiabatic electric field, the material's dipoles align, reducing polarization entropy and raising its temperature. Electric field removal reversibly disorders the dipoles, causing cooling (Fig. 2E).<sup>37,78</sup> From a device design perspective, the EC effect enables heat transfer through changes in the electric field, as shown in Fig. 2E.

When an electric field is applied to EC materials, heat is transferred from the material to a heat sink. Subsequent removal of the electric field after thermal exchange causes the EC material's temperature to decrease, enabling heat absorption from a source and thereby establishing refrigeration or heat pump functionality.<sup>79–81</sup> Compared to TE coolers, EC devices exhibit superior COP, enabling more efficient heat transfer per unit input electrical energy.<sup>82</sup> However, current EC materials still exhibit relatively small temperature changes under an applied electric field, resulting in inadequate cooling power compared to conventional refrigeration technologies.<sup>83</sup> From a materials science perspective, the intrinsically low thermal conductivity of EC polymers presents a fundamental limitation. This limitation results in insufficient thermal penetration depth during rapid heat exchange between the heat sink and the heat source, as well as excessively long thermal equilibrium time, which ultimately limits the improvement of cooling power. Furthermore, the requirement for high driving voltages (on the order of kV) raises substantial safety concerns for both human applications and electronic system integration. This

represents another critical barrier that must be overcome for widespread EC device adoption.

### 2.3 Mechanism of microfluidics-based thermal management

Commonly used natural cooling and forced air cooling methods are increasingly inadequate for addressing the thermal management challenges of high power-density, highly integrated flexible electronics. There is a pressing demand for thermal management solutions that offer efficient heat dissipation, compact form factors, and uniform temperature distribution. Microfluidic thermoregulation systems operate on the principle of heat transfer from the substrate to the working fluid flowing through the microchannels, which then carry the heat away from the device. Based on whether phase change occurs within the microchannels, microchannel cooling technologies can be categorized into single-phase cooling without phase change and flow boiling cooling with phase change.

In a microchannel single-phase system, the coolant remains in a liquid state throughout the refrigeration process without undergoing phase change reactions, primarily relying on the liquid's specific heat capacity for sensible heat exchange. The heat transfer process in this system is governed by forced convection, which is described by Newton's cooling law. The flow characteristics are primarily laminar, with the maximum velocity occurring at the centre of the channel, offering advantages such as high stability and precise temperature control.<sup>84</sup> However, this cooling system has a major drawback: when applied to large-scale electronic devices, the substantial temperature difference between the inlet and outlet of the microchannels causes the liquid to absorb heat continuously along the flow direction. This disadvantage can result in an obvious axial temperature gradient within the channel, leading to uneven temperature distribution across the chip surface. To improve temperature uniformity, a substantial increase in the coolant flow rate is often required. This not only significantly increases system energy consumption and pumping costs but also introduces additional issues, such as flow-induced noise and vibration, greatly increasing system complexity and maintenance costs.

Owing to its large specific surface area, flow boiling cooling technology has been employed to address hotspots with high heat flux. The liquid absorbs heat and vaporizes at hotspots, removing large amounts of thermal energy through latent heat absorption. The process involves the following steps: firstly, the heat source heats the inner wall of the microchannel, transferring thermal energy to the flowing liquid coolant. When the wall temperature exceeds the coolant's saturation temperature, nucleation sites form, generating vapor bubbles that grow and detach due to surface tension effects. Next, the bubbles mix with the liquid, forming a gas-liquid two-phase flow that absorbs significant latent heat through vaporization. Finally, the vaporized coolant releases its latent heat in the condenser, condenses back into liquid, and recirculates. Two key parameters define

the performance of boiling heat transfer: the critical heat flux (CHF), which represents the safe operational limit of nucleate boiling before film dryout and a sharp decline in heat transfer efficiency, and the heat transfer coefficient (HTC), which quantifies the heat removal rate per unit area.<sup>85</sup> However, in practical applications, CHF and HTC often exhibit a trade-off relationship, demanding co-optimization strategies that cover surface modification, microchannel design, and coolant selection.

The characteristics of microfluidic flow significantly influence heat transfer performance due to confined flow conditions and high surface-to-volume ratios. The two-phase flow behaviour is determined by the equilibrium established between inertial, viscous, and interfacial forces. The Reynolds number ( $Re$ ), a dimensionless parameter defining the ratio of inertial to viscous forces, determines flow regimes. Laminar flow ( $Re < 2000$ ) exhibits parallel fluid layers and minimal mixing that primarily enables heat transfer through conduction and weak natural convection. The thermal boundary layer, which describes a thin region near the channel wall with obvious temperature gradients, reduces the heat efficiency. For example, in straight microchannels with laminar flow, temperature gradients become pronounced downstream, leading to localized hotspots. Although laminar flow is efficient in minimizing energy loss, its lack of turbulent mixing severely limits convective heat transfer. This is particularly problematic in high heat-flux flexible electronics, where passive cooling solutions often fail to dissipate heat rapidly. In contrast, turbulent flow ( $Re > 4000$ ) generates chaotic vortices that disrupt the thermal boundary layer, significantly enhancing forced convection. The resulting fluid mixing produces a more uniform temperature distribution and can increase the heat transfer efficiency significantly compared with laminar flow. This turbulent transition dramatically improves thermal mixing, facilitating rapid heat dissipation of localized hotspots. However, turbulent flow requires high pumping power due to elevated friction losses, creating a design trade-off. While enhanced mixing improves heat dissipation, the accompanying pressure drop leads to greater energy consumption. This balance is especially crucial in flexible electronics, where power supply is a key constraint. Thus, researchers must carefully optimize the  $Re$  to maximize thermal performance without exceeding energy budgets.

## 3. Design strategies for microfluidics-based thermal management

### 3.1 Materials and fabrication

The performance of microfluidic systems in thermal management hinges critically on selecting appropriate materials. These materials must fulfil two requirements: mechanical compatibility with flexible electronics and efficient heat transfer capabilities. This section reviews microchannel materials and fluid media, investigating how their composition and fabrication process influence thermal

and mechanical performance by key parameters such as the aspect ratio, surface roughness, and solvent compatibility of channels.

**3.1.1 Microchannel materials.** The materials for microfluidic channels play a crucial role in determining the durability, flexibility and thermal conductivity of microfluidic systems. When selecting these materials, it is essential to comprehensively consider various factors, such as mechanical properties like tensile strength, elongation at break, and flexibility, as well as thermal conductivity. In applications where efficient heat dissipation is critical, materials with high thermal conductivity, such as certain polymers or advanced composites, are usually the preferred options. Chemical stability is another key aspect to assess, as the material must not react with the transported fluids. Moreover, biocompatibility is of great importance for biomedical applications. Additionally, the cost and processability of the material are practical factors that can influence the overall feasibility and scalability of the microfluidic system. Common materials utilized for this purpose include PDMS and thermoplastics.

PDMS is a silicone-based elastomer widely adopted in flexible microfluidics due to its excellent stretchability (up to 300% strain), biocompatibility, and optical transparency.<sup>86</sup> However, its low thermal conductivity limits passive heat dissipation, making it inapposite for the base material of microfluidic heat sinks.<sup>87</sup> Researchers have incorporated various thermally conductive fillers into PDMS matrices, such as BN nanosheets, alumina oxides, graphene powders, graphene oxide (GO), or carbon nanotubes (CNTs). Table 2 summarizes the thermal conductivities of commonly used functional fillers. Luo *et al.*<sup>88</sup> proposed a thermally conductive elastomer based on PDMS-GO nanocomposites by adding 5% weight fraction of GO nanoparticles, exhibiting 250% increased thermal conductivity and 200% higher elastic modulus compared to pure PDMS, while maintaining essential flexibility for microfluidic integration. He *et al.*<sup>89</sup> prepared PDMS-based composites with low-frequency microwave absorption properties and high thermal conductivity by incorporating functional fillers, CoNi and BN into PDMS. A spray-drying-sintering process is employed to assemble chain-like CoNi and flake BN into hydrangea-like CoNi@BN heterostructure fillers. When the volume fraction

of the filler is 44% and the mass ratio of CoNi to BN is 3:1, the in-plane thermal conductivity of the CoNi@BN/PDMS composites is  $7.3 \text{ W m}^{-1} \text{ K}^{-1}$ , which is about 11.4 times the thermal conductivity for pure PDMS, and 32% higher than that of the (CoNi/BN)/PDMS composites,  $5.5 \text{ W m}^{-1} \text{ K}^{-1}$ , with the same volume fraction of CoNi and BN obtained through direct mixing.

Thermoplastics, such as polystyrene, polycarbonate, cycloolefin copolymers, and polymethyl methacrylate (PMMA), are widely employed in microfluidic systems due to their tunable mechanical properties, cost-effectiveness, and compatibility with high-throughput manufacturing techniques. Unlike elastomers, thermoplastics offer superior stability under thermal cycling and mechanical stress, making them suitable for applications requiring precise channel geometries.

Most thermoplastics inherently possess low thermal conductivity (e.g., PMMA:  $0.17\text{--}0.25 \text{ W m}^{-1} \text{ K}^{-1}$ ,<sup>90</sup> polycarbonate:  $0.3 \text{ W m}^{-1} \text{ K}^{-1}$  (ref. 91)), limiting their passive heat dissipation capabilities. Researchers incorporate thermally conductive fillers such as BN, graphene, or CNTs into polymer matrices. For instance, Wu *et al.*<sup>92</sup> prepared h-BN/PMMA composites by *in situ* polymerization. Previously, such composites often face limitations due to poor particle dispersion in polymer matrices when prepared by melt mixing. To mitigate filler aggregation, incorporating inorganic powders into a viscous prepolymer has been proposed as an effective strategy. In this paper, h-BN/PMMA composites were prepared by *in situ* polymerization of methyl methacrylate with  $5 \mu\text{m}$  and  $20 \mu\text{m}$  h-BN particles. When the h-BN mass fraction reached 20 wt%, the thermal conductivity of the composites increased by 107% ( $5 \mu\text{m}$  h-BN) and 189% ( $20 \mu\text{m}$  h-BN), respectively. This work demonstrates a filler strategy for achieving uniform h-BN dispersion in polymer matrices, significantly enhancing thermal conductivity.

Kim *et al.*<sup>96</sup> enhanced the mechanical, electrical, and thermal properties of the substrate material PMMA through the incorporation of graphene. They developed a float-stacking strategy to precisely align monolayer graphene reinforcements within the polymer matrix. This approach involved floating a graphene-PMMA membrane at the water-air interface and then winding it layer-by-layer using a roller. When 100 layers of monolayer graphene were uniformly embedded in a PMMA matrix at regular intervals, the thermal conductivity reached about  $4 \text{ W m}^{-1} \text{ K}^{-1}$  with a 2000% enhancement compared to pure PMMA film.

**3.1.2 Media materials.** In the field of microfluidic technology, the selection of fluid media for microchannels is crucial and is affected by multiple factors. The physical properties of the fluid, like viscosity and surface tension, are of importance as they directly impact fluid flow dynamics and precision of fluid control in the microfluidic devices. The chemical compatibility between the fluid and the channel materials must also be carefully considered to prevent any adverse reactions that could compromise the integrity of the device or the accuracy of the analyses being conducted. The thermophysical properties of the fluid

**Table 2** Thermal conductivity of different fillers

| Functional fillers | Thermal conductivity, $\text{W m}^{-1} \text{ K}^{-1}$ | Ref. |
|--------------------|--|------|
| BN                 | 250–300  | 93   |
| Aluminum oxide     | 20–29  | 93   |
| Graphene           | 3080–5300  | 94   |
| CNTs               | 2000–6000  | 93   |
| Silicon nitride    | >150   | 95   |
| Silicon carbide    | >270   | 95   |
| AlN                | >260   | 95   |
| Aluminum           | 204  | 93   |
| Gold               | 345  | 93   |
| Copper             | 483  | 93   |
| Silver             | 450  | 93   |

medium become critically important in microfluidic applications involving heat transfer or precise temperature regulation. The biocompatibility of the fluid is another key factor, particularly in biomedical and biological research, to ensure that the fluid does not have any toxic or inhibitory effects on biological samples. Also, the fluid stability under the specific operating conditions of the microfluidic system, including temperature, pressure, and exposure to chemicals, must be assessed to guarantee reliable and stable performance over time. PCMs, aqueous solutions, and liquid metals represent three primary categories of functional media employed in microfluidic systems.

PCMs can absorb or release substantial latent heat during phase transitions. This property helps them to maintain a relatively stable temperature during phase changes, remaining near their phase change temperature during both endothermic and exothermic processes. Such thermal regulation is crucial for maintaining stable temperature in various systems. PCMs are generally classified into three main categories: organic, inorganic, and eutectics of inorganic and organic compounds. Table 3 provides a comprehensive summary of the properties of commonly-used PCMs. Organic PCMs commonly include paraffin wax and nonparaffin materials. Paraffin waxes are hydrocarbon mixtures primarily composed of linear alkanes with the general formula  $C_nH_{2n+2}$ , where  $n$  represents the number of carbon atoms. Notably, the melting point increases with hydrocarbon chain length. While paraffin waxes are safe, reliable, noncorrosive PCMs, they have low thermal conductivities. Similarly, non-paraffin organic materials like fatty acids, polyalcohols, and polymers (*e.g.*, polyurethane) also exhibit low thermal conductivity. In contrast, inorganic PCMs, including salt hydrates and metals/alloys, not only have higher thermal conductivity than organic PCMs but also demonstrate relatively smaller volume changes during melting. However, several inorganic PCMs pose human health and environmental risks, which impedes applications

in biomedical devices. Eutectic PCMs typically consist of two or more low melting-temperature components. Their advantage is that the phase transition point can be changed by adjusting the proportion of the components, which may also affect their heat storage capacity. The characteristically low thermal conductivity of PCMs fundamentally constrains their thermal performance.<sup>100</sup> The low thermal conductivity of pure PCMs severely limits heat transfer, causing slow thermal energy storage processes (both charging and discharging) and failure to provide stable temperature control in thermal management applications.

In cooling devices and industrial applications, convective heat transfer holds an integral position. The promotion of heat transport can be achieved through manipulating the boundary conditions, altering the flow geometry, or enhancing the thermophysical properties of the working fluids. A widely employed strategy involves dispersing metallic or metal oxide nanoparticles (1–100 nm) in base fluids, forming stable suspensions known as nanofluids.<sup>104</sup> The extra nanoparticles enhance the thermal conductivity of conventional liquids dramatically, leading to an improved heat transfer performance. However, the complexity of microfluidic chip fabrication methods often introduces challenges including structural defects, channel leakage, and non-uniform nanoparticle dispersion during nanofluid synthesis. Additionally, further investigation is required into the mechanisms by which nanofluids function as heat transfer media in improving the thermal management of electronic chips. This encompasses a more comprehensive understanding of their influence on bubble dynamics within flow boiling heat transfer processes. Some researchers have improved thermal conductivity by introducing nanofluids into base fluids. For example, Huang *et al.*<sup>105</sup> synthesized silver nanoparticles using microfluidic technology, achieving excellent colloidal stability (>60 days) and uniform nanoparticle size (<30 nm). The results demonstrated that silver nanofluids showed significant enhancements, with 0.01

**Table 3** Properties of commonly-used PCMs

| Compound   | Melting temperature/°C | Heat of fusion/kJ kg <sup>-1</sup> | Thermal conductivity/W m <sup>-1</sup> K <sup>-1</sup> | Ref. |
|--|------------------------|------------------------------------|--|------|
| MgCl <sub>2</sub> ·6H <sub>2</sub> O                 | 117                    | 168.6                              | 0.6 ( <i>l</i> )<br>0.7 ( <i>s</i> )                   | 97   |
| Mg(NO <sub>3</sub> ) <sub>2</sub> ·6H <sub>2</sub> O | 89                     | 162.8                              | 0.5 ( <i>l</i> )<br>0.6 ( <i>s</i> )                   | 97   |
| Ba(OH) <sub>2</sub> ·8H <sub>2</sub> O               | 77.9                   | 283.7                              | 0.7 ( <i>l</i> )<br>1.2 ( <i>s</i> )                   | 98   |
| CaCl <sub>2</sub> ·6H <sub>2</sub> O                 | 28                     | 180                                | 0.5 ( <i>l</i> )<br>1.1 ( <i>s</i> )                   | 99   |
| Paraffin wax   | 55                     | 210                                | 0.2 ( <i>l</i> )<br>0.4 ( <i>s</i> )                   | 100  |
| Palmitic acid  | 64                     | 185.4                              | 0.2 ( <i>l</i> )                                       | 101  |
| Capric acid  | 31.2                   | 173.8                              | —<br>0.2 ( <i>l</i> )                                  | 102  |
| PEG  | 60.4                   | 168.6                              | 0.2 ( <i>l</i> )<br>—                                  | 103  |

Note: *l* represents liquid and *s* represents solid.

wt% achieving a 66% increase in CHF and a 49.3% increase in HTC at a flow rate of 160 mL min<sup>-1</sup>. Zhao *et al.*<sup>106</sup> developed SiO<sub>2</sub> and TiO<sub>2</sub> nanofluids using a microfluidic device. The SiO<sub>2</sub> nanofluids demonstrated significant enhancements in CHF and HTC by 77% and 96%, respectively, while the TiO<sub>2</sub> nanofluids achieved 44% and 56% improvements in CHF and HTC. These findings not only provide insights into the industrial preparation of high-performance nanofluids but also advance thermal management strategies for high-power electronic devices.

Aqueous solutions, which mainly consist of water and water-based fluids, are extensively utilized in microfluidic thermal management. This is attributable to their advantageous properties such as high specific heat capacity, low viscosity, non-toxic nature, and biocompatibility. These properties enable efficient convective heat transfer while minimizing pumping power requirements. Water, with a specific heat capacity of ~4.18 kJ kg<sup>-1</sup> K<sup>-1</sup> and thermal conductivity of ~0.6 W m<sup>-1</sup> K<sup>-1</sup>, serves as a cost-effective baseline coolant. However, it has limitations including a relatively low boiling point (100 °C at 1 atm), freezing risk at 0 °C, and moderate thermal conductivity compared to engineered fluids.<sup>107</sup> To enhance its cooling efficiency, researchers have proposed various optimization schemes. For example, Tang *et al.*<sup>108</sup> designed a hybrid impinging microchannel heat sink. The results show that increasing jet-to-target spacing and mass flux and decreasing subcooling can improve the heat transfer coefficient, with the maximum heat transfer coefficients increasing by 58%, 73%, and 50%, respectively. Yet, the latest developments in micro- and nano-scale heat-transfer components may restrict the thermal efficiency of water-based systems in eliminating large heat fluxes from advanced electronic equipment. Consequently, researchers have proposed water-based nanofluid-based solutions. Waqas *et al.*<sup>109</sup> experimented with TiO<sub>2</sub>/water nanofluid as a coolant and found that when the mass fraction of TiO<sub>2</sub> rose from 1% to 3%, the HTC climbed from 12% to 14% higher than that of pure water.

Liquid metals possess a range of distinctive properties that have drawn plenty of attention for their potential applications in flexible electronics. Their exceptionally high thermal conductivity, coupled with inherent fluidity, enables efficient heat dissipation and precise temperature regulation in advanced thermal systems. For example, Deng *et al.*<sup>110</sup> investigated a two-stage multichannel liquid metal cooling system for a high heat flux-density chip array. The hybrid cooling system combines a multichannel liquid metal convection subsystem for efficient thermal management of high heat-flux-density chips with a water-cooling subsystem that provides cost-effective secondary cooling. Furthermore, each liquid metal circulation was equipped with an electromagnetic pump, which facilitated convenient adjustment of the chip temperature, thereby achieving desirable temperature uniformity. The experimental outcomes demonstrated that the heat transfer coefficient of the liquid

metal surpassed 20 000 W m<sup>-2</sup> K<sup>-1</sup>, and it was capable of handling a heat flux within the range of 50–200 W cm<sup>-2</sup>. Under the centralized control of the electromagnetic pumps, the temperature difference across the chip array was minimized to below 1 °C, with each individual electromagnetic pump consuming less than 0.2 W of power. Notably, its advantages such as high performance, excellent temperature uniformity, low power consumption, and cost-effectiveness render it a promising candidate for the thermal management of chip arrays in servers and data centers.

**3.1.3 Fabrication routes.** We group fabrication into soft lithography, stereolithography-based 3D printing, and hybrid molding. Each route ties to distinct material systems, solvents, and achievable geometries. Soft lithography, based on PDMS casting and molding, is the dominant fabrication method for microfluidic chips. However, its effectiveness in thermal management is constrained by PDMS's poor thermal conductivity, which impedes efficient heat dissipation. Recent progress has been made by optimizing photolithography, like adjusting SU-8 photoresist exposure and development to make high aspect-ratio microchannel molds (aspect ratios over 10). Chande *et al.*<sup>111</sup> developed an integrated approach combining SU-8 photolithography, 3D printing, and soft lithography. This technique involves 3D-printing SU-8 master molds, which are then replicated in PDMS to create smooth, high aspect-ratio microchannels. This strategy not only reduces hydrodynamic flow resistance but also significantly enhances heat transfer efficiency. Furthermore, the method permits the incorporation of thermally conductive fillers (Table 2) into PDMS, offering an effective route to improve its inherently low thermal conductivity.

3D-printed microfluidic heat sinks offer a promising solution for electronic hotspot thermoregulation by enabling precise design control.<sup>112</sup> This capability facilitates the fabrication of intricate geometries that enhance fluid–solid interaction, thereby maximizing heat transfer efficiency. Furthermore, microfluidic devices fabricated *via* 3D printing scaffold-removal techniques can integrate PDMS-nanocomposite heat sink materials,<sup>113</sup> significantly enhancing thermal conductivity for superior heat transfer performance. 3D printing can be divided into direct and indirect methods. Direct printing fabricates functional devices without molds, whereas indirect printing first produces a mold that is subsequently used for reverse molding with base materials.

Stereolithography (SLA), a vat photopolymerization technique, utilizes ultraviolet (UV) light to selectively cure liquid resins into high-resolution 3D structures. Renowned for its high precision (<20 μm feature size), SLA is suitable for fabricating complex microchannel geometries that maximize the fluid–solid interface contact area.<sup>114</sup> This capability is particularly advantageous for thermal management in flexible electronics, where spatially heterogeneous heat fluxes demand tailored cooling architectures.

While SLA-printed microfluidic devices typically exhibit mechanical rigidity due to the inherent brittleness of UV-curable resins, recent advancements have focused on combining SLA with elastomers to enhance flexibility. To further address thermal conductivity limitations, researchers have incorporated thermally conductive nanoparticles into UV resins or post-processed SLA structures with conductive coatings. Such modifications enhance passive heat transfer without compromising print resolution. Lorenzo *et al.*<sup>115</sup> investigated 3D-printed silicone-acrylate photocurable composites doping BN as a thermally conductive filler. Significant challenges still remain in simultaneously optimizing resolution, flexibility, and thermal conductivity in SLA-printed components. Additionally, multi-material SLA printing, essential for integrating rigid cooling components with soft substrates, requires further development to ensure interfacial adhesion and durability. Future directions include exploring dynamic-covalent resins for self-healing networks, bioinspired hierarchical channel designs, and hybrid manufacturing techniques (*e.g.*, combining SLA with soft lithography) to realize scalable, high-performance thermal management systems.

### 3.2 Design strategies of microchannels

Microfluidic technology offers a versatile platform for thermal management in flexible electronics, but its effectiveness heavily relies on structure design approaches. This section reviews key design strategies, including channel geometry optimization and advanced fabrication techniques, supported by material innovations and computational modeling.

The geometry of microfluidic channels directly influences heat transfer efficiency, pressure drop, and mechanical compatibility with flexible substrates. Key design considerations include serpentine channels and bionic topology. The serpentine channel is a typical microfluidic cooling structure that significantly enhances thermal exchange efficiency by prolonging the fluid path, which increases the contact time between the fluid and channel walls. Its design is characterized by a periodically meandering geometry, which effectively induces fluid mixing and reduces the thermal boundary layer thickness, thereby enhancing convective heat transfer. Al-Neama *et al.*<sup>119</sup> and Jaffal *et al.*<sup>120</sup> optimized the pump power loss and cooling



**Fig. 3** Bio-inspired cooling channel designs. (A) Nature physical objects: ternate vein, lateral vein, snowflake, and spider net<sup>116</sup> (reproduced with permission from ref. 116, Copyright 2019, Elsevier); (B) the corresponding microfluidic channels with bio-inspired design: ternate vein, lateral vein, snowflake shaped, and spider netted<sup>116</sup> (reproduced with permission from ref. 116, Copyright 2019, Elsevier); (C) a microfluidic channel modeled after a lung and a microfluidic channel modeled after a lotus leaf<sup>117</sup> (reproduced with permission from ref. 117, Copyright 2023, Elsevier); (D) biomimetic microchannels of blood vessels. Left is blood vessel, middle is biomimetic design of blood vessels, and right is thermal imagery<sup>118</sup> (reproduced with permission from ref. 118, Copyright 2019, Elsevier).

effect of the snake-like microchannel by studying the number of channels and the structure of the ribs. Additionally, serpentine microchannels have a high spatial utilization rate and can achieve uniform cooling. Among various designs, such as parallel channels, swirl channels, and channels with special shapes, serpentine channels exhibit higher comprehensive performance. Gorzin *et al.*<sup>121</sup> designed a novel serpentine microchannel heat sink for liquid CPU cooling. Through experimental and numerical analysis, they systematically evaluated the thermal-hydraulic performance under various operating conditions. The proposed maze serpentine microchannel consistently exhibits lower baseplate temperatures across all mass flow rates compared to the straight channel. Most significantly, it achieves an 11.2% reduction in base temperature at the maximum mass flow rate.

Compared to conventional parallel and serpentine channels, bio-inspired flow channels, modeled after natural bifurcated systems like trees, leaves, lungs, and blood vessels, offer benefits such as decreased pumping power and enhanced temperature uniformity. As shown in Fig. 3, bionic topology has been proposed and applied in microchannel cooling techniques to improve the heat dissipation effect.<sup>122</sup> Common biomimetic structures include tree-like structures, feather-inspired topological structures, river-inspired topological structures, spider web-inspired topological structures, and insect-venation inspired topological

structures. Xu *et al.*<sup>126</sup> designed a bio-inspired microchannel system with a tree-shaped topological architecture for thermal management in proton exchange membrane fuel cells. Tan *et al.*<sup>116</sup> investigated the impact of various microchannel topologies (triangular, lateral, snowflake, and spider) on chip cooling heat transfer performance using a combination of fluid-thermal coupled numerical simulations and experimental methods (Fig. 3A and B). Results indicate that the spider web microchannel exhibited the best heat transfer performance among the proposed structures. Notably, the topology of the microchannel, particularly under high heat flux conditions, significantly influences heat transfer performance. Trogadas *et al.*<sup>117</sup> and Li *et al.*<sup>118</sup> designed different microchannel structures inspired by the geometry of the lung and lotus leaf, respectively, which helps achieve more uniform heat distribution (Fig. 3C and D).

Raza *et al.*<sup>123</sup> conducted a comparative study of microchannel heat sinks, investigating both conventional and hybrid designs with pin-fin geometries of circular, hexagonal, pentagonal, square, and triangular. Cross-sectional profiles of all investigated pin-fin configurations are illustrated in Fig. 4A. To isolate the influence of pin-fin geometry, the cross-sectional areas of different configurations of fins were maintained equal to that of circular pin fins. These pin fins were torsional deformed at twist angles ranging from 0° to 360°. The hybrid heat sinks equipped with twisted pin fins outperformed their non-hybrid counterparts



Fig. 4 Pin-fin structural diagram. (A) Non-hybrid heat sink and hybrid pin-fin heat sink. (B) Microchannel geometric dimensions with hotspot zone enlargement. (C) Twisted and non-twisted pin-fins<sup>123</sup> (reproduced with permission from ref. 123, Copyright 2024, Elsevier). (D) The investigation of the microchannel heat sink with sidewall square pin-fins<sup>124</sup> (reproduced with permission from ref. 124, Copyright 2025, Elsevier). (E) Oblique microchannel merged with a circle micro pin-fin.<sup>125</sup> (F) The temperature contours in three transverse sections of case V<sup>125</sup> (reproduced with permission from ref. 125, Copyright 2024, Elsevier).

as shown in Fig. 4B. Both non-twisted and twisted pin-fin geometries influenced the performance of hybrid heat sinks, with triangular pin fins showing the greatest enhancement. In addition to periodically disrupting the thermal boundary layer, the twisted pin fins generated three-dimensional secondary flow, enhancing fluid mixing and thereby improving heat transfer. The twist angle's impact on the hybrid heat sink's thermal-hydraulic performance was closely tied to the pin-fin geometry (Fig. 4C). As the pin-fin shape evolved from hexagonal to pentagonal, square, and triangular, the thermal performance metrics showed a continuous upward trend. This was mainly because the flow-sweeping area increased with twisting. Notably, among all the shapes, the triangular pin-fin exhibited the most significant variation in performance with changes in the twist angle. Alnaimat *et al.*<sup>124</sup> investigated straight microchannel heat sinks with square fins integrated on the sidewalls (Fig. 4D). The integration of square fins enhanced cooling performance, with an increase in fin size and a decrease in channel spacing reducing the thermal resistance by an average of 53.5% and 62.2%, respectively. Alihosseini *et al.*<sup>125</sup> designed a novel hybrid heat sink for electronic-device cooling by integrating inclined microchannels with circular micro pin-fins, and evaluated its cooling performance. This study investigates the effects of hybrid designs on electronic chip cooling by combining microchannel and pin-fin patterns. The research contrasts the performance of a straight microchannel heat sink (case I), circular pin-fin (case II), straight-circular pin-fin-straight (case III), and oblique grooved straight-circular pin-fin-oblique grooved straight (case IV). To achieve a more uniform thermal distribution across the entire heat sink, the orientation of the oblique grooves is modified in case IV, resulting in a new design labeled case V (Fig. 4E). Simulation results indicate that the contrasting orientations of the inlet and outlet grooves in case V contribute to its superior temperature uniformity and lower operating temperatures (Fig. 4F).

## 4. Applications of microfluidics-based thermal management

The integration of microfluidics for thermal management has expanded its scope beyond the conventional goal of cooling electronics under extreme conditions, enabling broader applications in flexible and wearable systems.<sup>74,127</sup> Utilizing the key features of flexible electronics, such as lightweight, and excellent stretchability, microfluidic thermal management systems can now cool biological surfaces like the skin, tissues, and organs. Consequently, thermal regulation is no longer solely a means of enhancing system reliability but has also acquired distinct functional roles.<sup>31</sup> In this review, we categorize these applications based on the primary objective of the thermal management strategy. This section begins with device-level thermal management, which is fundamental to ensuring electronic performance and reliability. This is followed by personal thermal regulation,

which focuses on regulating human comfort. Finally, we present thermal regulation interface for HMI and healthcare applications, an emerging field where the precise thermal control offered by microfluidics enables novel capabilities such as thermal haptic feedback and pain blockade.

### 4.1 Device-level thermal management

The rapid advancement of flexible and wearable electronics has significantly increased the integration density and power consumption of key components (*e.g.* processors, LEDs, and batteries), leading to a substantial increase in heat generation.<sup>128</sup> The resulting high heat flux causes the temperature of these electronic devices to soar, which severely degrades their performance, reliability, and operational lifetime. Therefore, achieving efficient heat dissipation at the device level has become a critical challenge. Microfluidic thermal regulation technology, characterized by its high cooling efficiency, uniform temperature distribution, and compact structure, has demonstrated great potential for addressing this issue in flexible electronics.

The first microfluidic cooling devices were microchannel heat sinks, consisting of microchannels fabricated on silicon chip substrates with hydraulic diameters of 10–30  $\mu\text{m}$ . These microscale features provided both a high surface area-to-volume ratio and low thermal resistance for enhanced heat transfer.<sup>129</sup> However, an external pressure source for the liquid supply is essentially unsuitable for compact embedded systems. Therefore, there is still a technological gap and an urgent need for integrated circuit cooling. Mukherjee *et al.*<sup>130</sup> developed a microfluidic cooling method with a pumpless loop. The technique relies on the difference in fluid density between two perpendicular parallel pipes to induce fluid movement, does not require an external pump, and the flow rate increases with increasing temperature. This passive cooling method requires no external electrical power supply.

Krishnendu *et al.*<sup>131</sup> proposed a technology to achieve adaptive cooling of integrated circuits using digital microfluidics, using the electrowetting phenomenon to achieve independent manipulation of discrete droplets, solving the problem that traditional continuous flow microfluidic architectures experience difficulty in coping with changes in the thermal distribution of integrated circuits. This method forms a fully reconfigurable system by independently moving a large number of droplets without the need for traditional components such as pumps and valves, thereby reducing complexity and cost. Dinh *et al.*<sup>132</sup> proposed a silicon carbide (SiC)-based system-on-chip that successfully integrated heating, sensing, and cooling functions. Taking advantage of the high thermal conductivity and excellent electrical properties of SiC thin films, they prepared a transparent heater and temperature sensor by growing SiC thin films on a silicon substrate and transferring them to a glass substrate. The heating and sensing components were formed using a MEMS process, and the

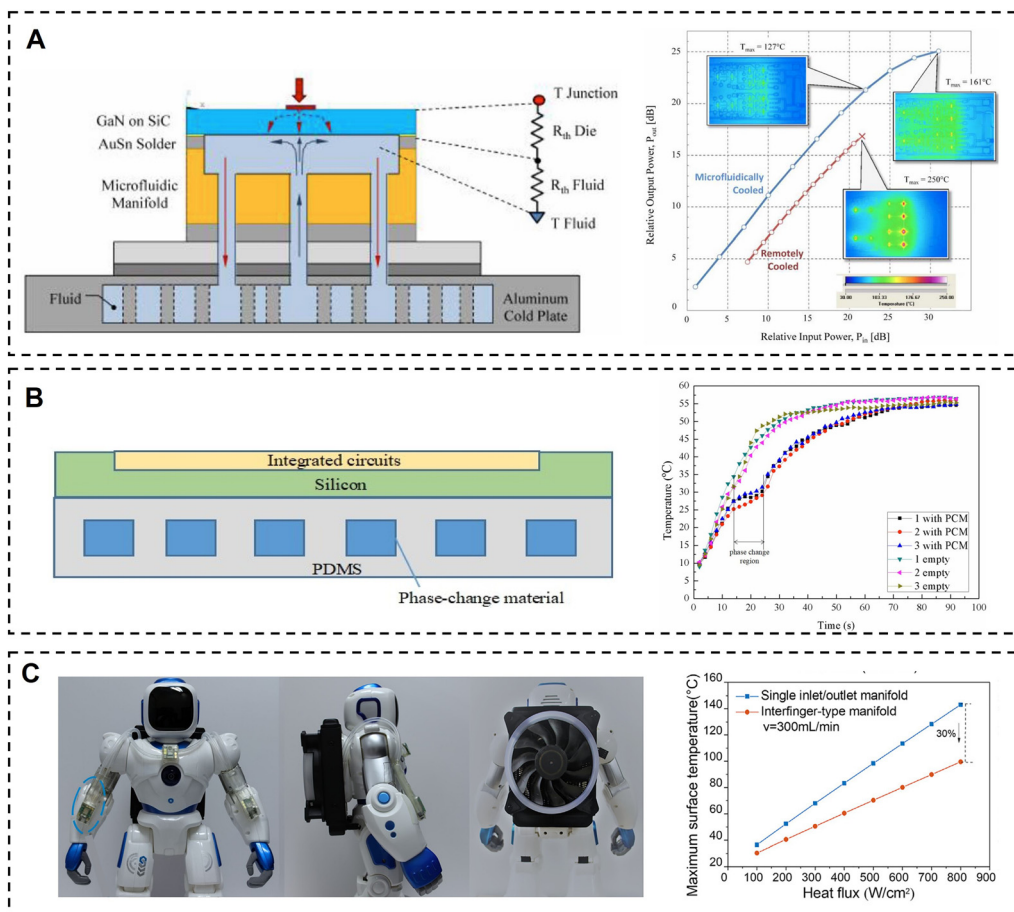


**Fig. 5** Microchannel-based cooling systems for electronic components. (A) Schematic representation of the embedded cooling concept (left). Comparative radiofrequency power output between conventional and microfluidics-cooled high-power amplifiers (right).<sup>133</sup> (B) A schematic diagram of the PDMS-based microfluidic device filled with PCMs for chip cooling in integrated circuits (left). The temperature variation of the three empty chips and three chips with PCMs over time (right)<sup>135</sup> (reproduced with permission from ref. 135, Copyright 2024, Elsevier). (C) Photographs of the flexible cooling modules (left). Effect of cooling modules on maximum temperature (right)<sup>136</sup> (reproduced with permission from ref. 136, Copyright 2024, Elsevier).

microchannel cooling system was fabricated by 3D printing, molding, and plasma-assisted bonding techniques. By applying a voltage of 2–3 V, the temperature of the SiC chip can be raised to 100–150 °C and effectively cooled by a microfluidic cooling system. In addition, the cooling effect increased with the increase in chip temperature, indicating that the system has good thermal management capabilities under high-power operating conditions.

Ditri *et al.*<sup>133</sup> developed an embedded microfluidic cooling technology to address the thermal management issues caused by the high-power density of gallium nitride (GaN) transistors. By setting up a series of microchannels, the coolant is sprayed directly onto the chip surface, significantly reducing the thermal resistance between the chip and the heat sink (Fig. 5A). This technology uses a multilayer additive manufacturing process and uses pure palladium material to manufacture the microchannel. Experimental results show that compared with traditional remote liquid cooling, microfluidic cooling technology increases the gain of GaN single-chip microwave integrated circuit amplifiers by more

than 4 dB, and the maximum output power by more than 8 dB. Wan *et al.*<sup>134</sup> used microfluidic cooling to cool a working CMOS chip to achieve better performance. Compared with natural air cooling, the temperature was reduced by 18.8 °C and the leakage current was saved by 66.2% at a heat flux of  $34.5 \text{ W cm}^{-2}$ .

Liu *et al.*<sup>135</sup> proposed a chip cooling scheme using PDMS microchannels filled with PCMs. They used SU-8 photoresist as a mold, fabricated microchannels using MEMS technology, and sealed the microchannels using thermocompression bonding technology. The phase change material *n*-octadecane was successfully filled into the microchannels, and its high ability to absorb and release heat significantly reduced the chip temperature (Fig. 5B). Under the same heating conditions, the microchannel device filled with *n*-octadecane can reduce the chip temperature by about 16 °C, showing excellent cooling performance. This flexible microfluidic device can be used for thermal management of flexible displays, electronic skin, and wearable devices. Researchers have investigated different cooling media to improve cooling

efficiency, including liquid metal,<sup>137</sup> water,<sup>138</sup> dielectric fluid,<sup>139</sup> *etc.* As an ideal material, water is considered to be the cost-effective cooling medium due to its low price, non-toxicity, and high thermal conductivity. Yang *et al.*<sup>140</sup> proposed that serpentine microchannels can maximize the operating performance of high heat flux density chips and reduce chip temperature by up to 55.1%.

With the advancement of sensor and AI technologies, humanoid robots are rapidly transitioning from laboratories to commercial applications, expanding applications to home services, education, and entertainment. However, the complex motion control of multi-degree-of-freedom joints in humanoid robots, combined with the integration of AI technologies like large language models (*e.g.*, ChatGPT), has led to an exponential increase in data computation and processing demands. Therefore, breakthroughs in efficient thermal management technology to ensure the stable operation of high-performance chips have become a crucial prerequisite for scaling the deployment of humanoid robots. To address this challenge, Du *et al.*<sup>136</sup> developed a flexible cooling manifold with embedded microchannels. This device could facilitate the heat transfer between multiple hotspots in a humanoid robot. The manifold incorporates a gradient stiffness design to bear the induced stress during joint twists and motion (Fig. 5C). Experimental results demonstrate a 30% decrease in maximum temperature compared to a single-inlet/outlet manifold as shown in Fig. 5C.

#### 4.2 Personal thermal regulation

Personal thermal regulation represents a shift from cooling electronic components to directly regulating human body temperature for enhancing comfort.<sup>142,143</sup> Textile and wearable systems, which serve as the critical interface for human–environment energy exchange, have witnessed great progress in the field of thermal radiation, fabrication methods and perspiration.<sup>25,144</sup> However, the integration of electronic functionalities often leads to unwanted heat accumulation, disrupting the thermal state of skin and causing discomfort. Microfluidics-based systems have emerged as a powerful solution for this application. Their ability to dynamically absorb excess body heat or provide localized heating enables precise thermal regulation, thereby significantly expanding the comfort and functionality of wearable technologies.

Smart textiles with thermal regulation systems are engineered to dynamically monitor human biomechanical activity and physiological status, enabling instantaneous feedback through adaptive signal modulation.<sup>145</sup> However, persistent heat generation during device operation critically compromises user comfort and long-term functionality.<sup>146</sup> Microfluidics-based intelligent fiber systems exhibit autonomous thermoregulatory properties, enabling environmental responsiveness to sustain continuous thermal comfort across wearable electronics and healthcare applications.

The human body regulates its temperature through perspiration as part of homeostasis. Zhang *et al.*<sup>147</sup> developed fabric-based microfluidic devices featuring oval-shaped reservoirs and 800  $\mu\text{m}$ -wide microchannels to investigate sweat delivery efficiency. They saturated reservoirs with blue dye, followed by controlled washing cycles using artificial sweat at physiological flow rates (3, 5, and 10  $\mu\text{L min}^{-1}$ ). Residual pigment quantification *via* time-dependent absorbance spectroscopy (630 nm) revealed over 95% removal within 2 min at 10  $\mu\text{L min}^{-1}$ . These results validated the efficient turnover of liquid samples in the microfluidic reservoirs, thereby enhancing an individual's thermoregulation capacity.

Beyond serving as an effective mechanism for perspiration transport in thermoregulation, microfluidic systems can be synergistically integrated with microfibrinous phase change materials to achieve smart textile thermal management functionality through precise regulation of microcapsule flow dynamics and dimensional parameters.<sup>148</sup> Wen *et al.*<sup>149</sup> engineered core–shell phase change microfibers with Rubitherm27 cores and poly (vinyl butyral) (PVB) encapsulation through microfluidic technology. The fabricated microfibers demonstrated stable and repeatable thermal regulation performance across multiple thermal cycles (16–40 °C) and under simulated solar irradiation. Utilizing thermoplastic frames as structural supports, two prototype hats were constructed through PVB and PVB/Rubitherm27 microfiber winding. Comparative thermal characterization revealed that the composite microfiber-integrated headgear exhibited 5.1 °C lower average surface temperature during heating phases and 4.6 °C higher retention during cooling phases *versus* the pure PVB counterpart. Under simulated solar conditions, the maximum inter-device temperature differential reached 3.6 °C. These findings establish fundamental design principles for microstructure-controlled phase change fiber engineering with optimized thermal management capabilities.

Hu *et al.*<sup>150</sup> fabricated an integrated smart textile by utilizing multiscale disordered porous elastic fibers as sensing elements through microfluidic spinning technology, endowing the material with dual functionalities of self-sensing and passive radiative cooling. The multiscale disordered porous architecture within the fibers enhances mid-infrared transmittance for human body radiation while simultaneously generating visible light backscattering. This synergistic optical modulation mechanism reduces the microenvironmental temperature between skin and textile by at least 2.5 °C compared to conventional cotton fabrics, thereby demonstrating superior self-cooling performance. Li *et al.*<sup>153</sup> fabricated sandwich-structured fabrics for personal thermal management *via* a facile and scalable method of microfluidic blow spinning and chemical vapor deposition. These fabrics integrate dual-mode thermal regulation capabilities: passive radiative cooling originating from a photonic crystal layer and active heating enabled by a nano-Ag layer, achieved through precise photonic bandgap

modulation and controlled voltage application. The passive radiative cooling mechanism demonstrates enhanced efficacy over conventional cotton fabrics, achieving a maximum absolute temperature differential of 7.9 °C.

Recent advances in micropumps have opened new possibilities for microfluidics-based thermoregulation cloth. A breakthrough innovation involves fiber-based pumps that utilize continuous helical electrodes along elastomeric tube walls, generating hydraulic pressure through charge-injection electrohydrodynamics.<sup>141</sup> As illustrated in Fig. 6A, the fiber pumps are capable of producing continuous flow without moving parts. Their unique design offers particular advantages for wearable applications, especially when integrated with microfluidic thermal management systems. Fig. 6B demonstrates the application of fiber pumps in thermal active textiles. The whole system is powered by a battery with low energy consumption and generated Joule heating.

### 4.3 Thermal regulation interface for HMI and healthcare

**4.3.1 Thermal haptics for HMI.** In virtual reality applications, the reproduction of thermal sensation is very important, and users can feel virtual objects with various thermal properties using thermal haptic feedback.<sup>11,154</sup> Thermal interfaces should be able to produce a wide range of temperatures above and below the average human body temperature, while accurately and quickly achieving the desired temperature. There are many ways to achieve the thermal haptic feedback, and Huang *et al.* summarized the implementation methods.<sup>58</sup> This part focuses on the method of using microfluidics to achieve the thermal haptic feedback. Microfluidic thermal management is a way to achieve two-way thermal haptic feedback (Fig. 7A). It uses conduction and convection of fluids in microchannels to cool or heat the target surface, which can cool or even heat the human body.<sup>151</sup> It is an effective thermal haptic feedback for virtual reality.

Yan *et al.*<sup>62</sup> developed a wearable thermal management system using 3D flexible microfluidic technology. The device is based on a gallium-based microfluidic channel, which is applied to the wrist and allows 0 °C cold water to circulate in the channel, thereby cooling the skin surface (Fig. 7B). At a flow rate of 1.75 ml min<sup>-1</sup>, the average temperature of the skin surface dropped from 35.3 °C to 20.3 °C. Goetz *et al.*<sup>155</sup> developed a pump-actuated thermal and compression haptic device. The device uses water of different temperatures to provide thermal tactile feedback. By mixing the ratio of water in the cold tank and the hot tank in the flow channel, temperature feedback ranging from 17 °C to 42 °C can be provided to the user. The system presents both thermal and compression cues simultaneously, providing a reference for the development of multimodal tactile devices.

Kotagama *et al.*<sup>152</sup> developed a soft, thermally conductive silicone aluminium composite tube that cools the body through water circulation for temperature regulation. The tube contains both aluminium powder and silicone elastomer to increase the thermal conductivity between the garment and the skin surface as shown in Fig. 7C. In addition to significantly improving the overall cooling capacity, the use of low-resistance pipes can also reduce the size of the cooling system by several times, providing a miniaturized approach for future applications of fluid temperature control methods. In addition to using aqueous fluids, Cai *et al.*<sup>156</sup> used air as a medium and developed a thermal haptic glove to reproduce the sensation of hot and cold by inflating the airbag with hot and cold air. The glove can provide five different levels of thermal perception and can reproduce the thermal sensation of different materials such as foam, glass, and copper. The average accuracy of users in material recognition of foam, glass, and copper was 87.2%. The user experience of using the proposed glove can significantly improve the user's sense of immersion in a virtual reality scene, compared to the case without any temperature or material simulation.



Fig. 6 Fiber pumps for wearable fluidic systems. (A) A soft fiber-format electrohydrodynamic pump. (B) A thermal regulation glove with fiber pumps.<sup>141</sup> Copyright the American Association for the Advancement of Science 2023 (reproduced with permission from ref. 141, Copyright 2023, the American Association for the Advancement of Science).



**Fig. 7** Microfluidics-based systems for personal thermoregulation. (A) Active thermal regulation strategies via microfluidic cooling<sup>151</sup> (reproduced with permission from ref. 151, Copyright 2023, Springer). (B) Schematic of the microfluidics-based cooling device for pain relief through peripheral nerve activity blockade (left). Infrared images of the microfluidic cooler during operation (middle). The microfluidic cooler sticking on the human arm for local cooling (right)<sup>62</sup> (reproduced with permission from ref. 62, Copyright 2023, Elsevier). (C) Illustrations of thermal-conductive composite liquid-cooling tubes.<sup>152</sup> An upper body liquid-cooled jacket layout (left). Outlet water temperature ( $T_{m,out}$ ) and total heat removed ( $Q$ ) as a function of the tubes' length ( $L_{tube}$ ) (middle and right) (reproduced with permission from ref. 152, Copyright 2019, John Wiley and Sons). (D) Adaptive robotic skin.<sup>15</sup> Schematic of robot E-skin (left), infrared images (middle) and the corresponding temperature changes on the robotic skin during soft-to-rigid conversion (right) (reproduced with permission from ref. 15, Copyright 2022, John Wiley and Sons).

The excellent conformability of E-skins makes them an essential platform for HMI.<sup>157–160</sup> However, the flexible polymer substrate often leads to significant heat generation in electronic components. In order to achieve thermal management of electronic skin, microchannels need to be connected to the outer surface of devices. By injecting cooling or heating fluid and flowing it through the channel, heat flow is generated between the target surface and the fluid. Researchers achieve bidirectional thermal management by simply replacing fluids of different temperatures or utilizing phase changes of fluids. The bidirectional thermal management mechanism helps to achieve the long-term application of electronic skin. Lee *et al.*<sup>15</sup> made a capacitive sensor consisting of two electrodes and a dielectric sandwiched between them, as shown in Fig. 7D. The dielectric layer is composed of an elastomer embedded with gallium particles, which is used as a sensing performance converter to achieve two electronic skins with different capacitive sensing capabilities by undergoing a phase change

between liquid and solid. When the particles are in a solid state, the capacitive sensor can have a larger pressure detection range. Conversely, when the particles are in a liquid state, the sensor can have a higher sensitivity. The thermal management device used is a microfluidic channel filled with water. The target temperature can be easily changed by simply changing the water temperature in the microchannel, thereby easily controlling the phase state of the gallium particles by replacing them with water of different temperatures (Fig. 7D). Park *et al.*<sup>161</sup> designed a hydrogel with good cooling ability based on the heat dissipation mechanism of human sweat secretion. Its micron-scale pores form microfluidic channels, which promote internal liquid circulation and evaporation through the capillary effect. The evaporation rate of the device at room temperature and 40 °C is 130% higher than that of stimuli-responsive hydrogels. Erp *et al.*<sup>18</sup> proposed to co-design microfluidics and electronics onto the same semiconductor substrate to produce a monolithic integrated manifold microchannel cooling

structure, considering that electronics and refrigeration are handled in two parts. Experimental results show that a heat flux of more than  $1.7 \text{ kW cm}^{-2}$  can be cooled using a pump power of  $0.57 \text{ W cm}^{-2}$ . This technology is expected to be combined with electronic skin technology to reduce the temperature rise caused by compact structural design. Hu *et al.*<sup>162</sup> proposed a flexible packaged phased array using microfluidic channels for cooling. Microfluidic cooling can effectively alleviate the temperature rise of IC chips. This low-temperature IC alignment method can be used for wearable devices, electronic skin, and smart applications. The above technologies provide technical support for the commercial application of microfluidic refrigeration for electronic skin.

**4.3.2 Healthcare applications.** Due to advancements in microelectronics and biomedical engineering, microchannel-based localized cooling devices have demonstrated broad application prospects in biomedical devices. Effective thermal management at the tissue level is critical for tissue engineering, wound healing, and pain relief, while also enhancing the reliability and precision of diagnostic and monitoring systems.<sup>163–165</sup> With the evolution of thermal management technologies, the focus of cooling strategies has

shifted from pursuing high thermal efficiency to developing lightweight, compact, and interface-integrated thermal management systems, particularly those that account for the biomechanical properties of biological tissues. For instance, next-generation bioelectronic cooling solutions designed for medical devices and home-based applications must operate effectively under tissue mechanics and large deformations, maintaining both heat transfer efficiency and cooling performance while ensuring conformal integration with soft tissues.<sup>167,168</sup>

In clinical practice, rapid tissue cooling technology has broad applications, including localized pain management, mitigation of adverse reactions, inflammation reduction, and hemorrhage control. While thermoelectric cooling and similar active methods can lower tissue temperature, these approaches rely on external energy input, resulting in bulky implantable devices, biosafety concerns, and external power dependence. Another critical consideration is precise control over the cooling area and depth, as excessive cooling can damage healthy tissue. Thus, targeted cooling must be confined to specific regions without affecting surrounding physiological functions. Reeder *et al.*<sup>61</sup> developed an

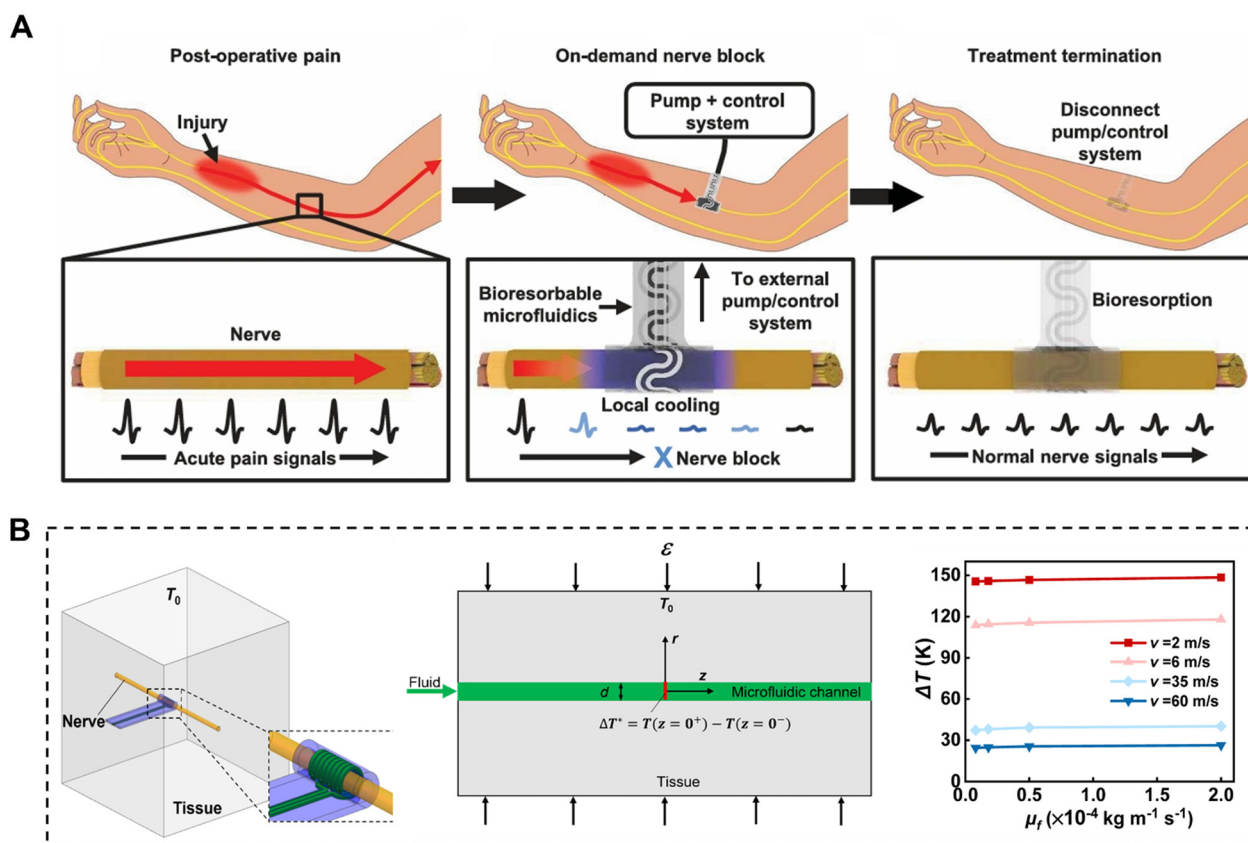


**Fig. 8** Microfluidics-based cooling systems for bioelectronic applications. (A) Bioresorbable microfluidic nerve coolers for on-demand pain management.<sup>61</sup> The left figure is transmission of postoperative acute pain signals through peripheral nerves. The middle one is localized nerve cooling that induces reversible conduction block. The right one is device dissolution upon tissue healing completion (reproduced with permission from ref. 61, Copyright 2022, the American Association for the Advancement of Science). (B) 3D model of the nerve wrapped by the microfluidic cooler, theoretical model of the microfluidic cooler inside the tissue, and temperature change for different flow rates.<sup>166</sup> The left figure is a 3D model of the nerve. The middle one is a theoretical model of the microfluidic cooler inside the tissue. The right figure is the temperature change for several flow rates (reproduced with permission from ref. 166, Copyright 2024, Elsevier).

implantable, biodegradable peripheral nerve cooling device for pain management (Fig. 8A), utilizing microfluidic PCMs to absorb heat and block neural signals. The system delivers dry nitrogen and perfluoropentane (PFP) liquid into a serpentine evaporation chamber, where PFP evaporates at room temperature, absorbing significant heat. The nitrogen then carries the cooled vapor through the microchannels to enhance cooling. The entire device is made of water-soluble and biocompatible materials, enabling post-treatment biosorption without additional surgery, thereby minimizing patient pain and risk. With integrated temperature monitoring, it effectively lowers nerve temperature in rat models, achieving reversible peripheral nerve blockade for localized analgesia.

Based on this work, Xie *et al.*<sup>166</sup> developed a theoretical model to study how flexible tissue and microchannel deformation affect viscous flow heat transfer, enabling precise spatial control over tissue temperature *via* phase-change cooling. As shown in Fig. 8B, their phase-change theory framework determines optimal fluid and gas inlet velocities to achieve targeted cooling in bioelectronic devices. Rapid localized cooling has also been applied in anesthesia and epilepsy suppression. Kim *et al.*<sup>169</sup> designed a cryotherapy-based platform integrating thermoelectric coolers and multi-electrode arrays. Neurons on the device surface exhibited safely reversible inhibition upon rapid cooling at  $20\text{ }^{\circ}\text{C s}^{-1}$ , while adjacent neural networks remained functional. This platform holds promise for combined use with chemical or optical neuromodulation, enabling sophisticated neural control for anesthesia and epilepsy treatment.

Beyond the aforementioned biomedical applications, microfluidics-based thermal management technology is poised to play an increasingly vital role in body temperature-regulated therapies, such as therapeutic hypothermia and wound temperature modulation.<sup>170</sup> Due to its precise thermal control capabilities, microfluidic systems can dynamically adapt to physiological temperature variations. The feasibility of such applications has already been demonstrated in thermoelectric or radiative cooling devices. For instance, contact-based thermoelectric coolers have been employed in treating acute ocular conditions, where therapeutic cooling alleviates pain and inflammation.<sup>171</sup> Similarly, radiative cooling dressings have been shown to reduce thermal load on sun-exposed wounds, accelerating healing processes.<sup>163</sup> Drawing inspiration from these cases, microfluidic thermoregulation technology holds significant potential for broader adoption in bioelectronics, particularly where precision temperature regulation and biocompatibility are paramount. In the future, microfluidics-based thermoregulation can utilize its advantages of mechanical flexibility, degradability, and high integration to develop precise temperature control devices for the nervous system. At the same time, it can be combined with thermoelectric devices to solve the problem of difficult waste heat discharge and explore its clinical translational capabilities.

## 5. Challenges and outlook

### 5.1 Challenges

Microfluidics-based thermal regulation systems have emerged as a promising solution for dynamic temperature control in flexible electronics. Although significant progress has been made in this field so far, there are still key challenges that need to be addressed. Looking toward the future, the fundamental materials, integration strategies as well as application scenarios should be concentrated to advance this technology.

Fundamental materials play a pivotal role in determining heat transfer performance in microfluidic devices. While significant progress has been made in developing high thermal conductivity polymer composites, substantial interfacial thermal resistance remains a critical barrier that impedes efficient heat conduction from thermal sources to cooling fluids. To enhance thermal transfer efficiency, it is essential to optimize both the conformal design of microfluidic cooling systems and novel strategies for improving thermal conductivity. The pursuit of higher thermal conductivity remains an ultimate objective, though this must be balanced against potential compromises in mechanical flexibility. Moreover, constructing three-dimensional thermal conduction pathways represents a crucial approach for facilitating rapid heat spreading in both vertical and horizontal directions within the matrix. Future strategies for constructing these pathways should focus on external field-induced alignment of fillers, bioinspired structural designs, as well as synergistic optimization of mechanical and thermal properties.

Future development of fluid media should focus on efficient cooling performance and environmental safety. The priority is to develop fluids with high thermal conductivity, low viscosity, and high stability, which will enhance thermal management efficiency and reduce system energy consumption. Research should aim to develop nanoparticles with excellent stability and dispersibility, utilizing surface modification techniques to avoid sedimentation and clogging. Additionally, attention should be paid to novel fluid types, such as PCM slurries. Based on the principles of latent heat storage and fluid transport, these fluids combine the flowability of single-phase fluids with the high energy storage capacity of two-phase systems, offering promising advancements in thermal management technology. Particularly for biomedical applications, it is paramount to consider biological safety and compatibility, with special emphasis on developing high-performance, bioresorbable fluid media to enable future implantable applications. Research should also explore the use of biological alcohols, castor oil, and similar substances as base fluids to enhance both environmental compatibility and biological adaptability.

The integration of microchannel-based methods with other thermal management technologies represents a key advancement. A prominent example is the hybrid system combining microchannels with phase change cooling, where

microchannels enhance heat transfer efficiency while PCMs provide a high latent heat absorption. This synergistic approach can be extended to systems incorporating TE materials, offering obvious advantages. On the one hand, microchannels can dissipate heat from the hot side of thermoelectric elements, leveraging their large surface area to mitigate heat accumulation and improve the COP of thermoelectric cooling devices. On the other hand, thermoelectric units can actively heat or cool the fluid media within microchannels, providing precise temperature control for personalized thermal regulation systems.<sup>172</sup> Beyond these strategies, emerging hybrid systems show great potential. For instance, microchannels coupled with electrocaloric cooling have demonstrated effective refrigeration in capillary systems.<sup>81</sup> Future developments could employ hollow electrocaloric material tubes as microchannel substrates, enabling compact, tunable thermal management platforms. Another innovative direction involves integrating microchannels with radiative cooling materials. Utilizing flexible radiative coolers with high infrared emissivity and solar reflectivity, the fluid media can achieve passive cooling, significantly reducing energy consumption while maintaining thermal regulation performance.

Thermal management for flexible electronics also presents unique challenges that require careful consideration of mechanical properties in the design of wearable and implantable microfluidic devices. While soft lithography produces microfluidic systems with good flexibility and stretchability,<sup>173</sup> epidermal electronics impose even greater demands on stretchability. A notable example is human skin over joints, which can experience tensile strains of up to 30%.<sup>174</sup> Structural integrity under stretching is another critical performance, as cracking could lead to liquid leakage, resulting in device failure and potential risks to the user.<sup>175</sup> Furthermore, the deformation of microchannels significantly influences fluid dynamics. For instance, the geometric changes directly modify key flow parameters, including fluid velocity, pressure, and flow resistance.<sup>176</sup> It is therefore critical to conduct quantitative investigation on thermal management performance.

For microfluidic systems, bending induces both tensile and compressive stress within the material, which can lead to undesirable fluid behaviours such as vortex formation, flow disturbance, and bubble entrapment. More critically, these stresses pose a threat to mechanical integrity by causing interfacial delamination between functional layers, which severely impairs long-term reliability.<sup>177</sup> In addition, microchannels with flat cross-sections are particularly susceptible to collapse and occlusion at small radii of curvature. To enhance the bending performance of microchannels, a commonly employed strategy is to position them at the neutral mechanical plane of the device, where tensile and compressive strains are minimized.

For microfluidic systems in flexible electronics, biocompatibility and biosafety are fundamental to ensuring reliable long-term operation. In addition to the substrate in

direct contact with skin or tissue, potential hazards caused by working fluid leakage must also be considered. Therefore, it is essential to use non-toxic and non-irritating working fluids. For implantable microfluidic devices, excellent degradability ensures complete degradation within the body, thereby eliminating the need for secondary surgical removal and preventing associated patient trauma.<sup>178,179</sup>

Barrier performance, defined as the ability of an encapsulation material to block moisture vapor and gases, is essential for the long-term stability and thermal management performance of microfluidic systems. A significant challenge is that most flexible polymers are permeable, allowing water vapor to continuously evaporate through the encapsulation into the atmosphere,<sup>4</sup> while working fluids may degrade due to solvent evaporation. On the other hand, materials with high barrier properties may cause sweat accumulation between the device and the skin, leading to redness and inflammation. A promising approach involves embedding a thin, impermeable layer into the inner wall of the microchannel, which can effectively block moisture transmission without significantly increasing the overall stiffness of the device.

## 5.2 Outlook

While microfluidics-based systems show great potential for thermal regulation, their capabilities remain underexplored, offering opportunities to utilize their unique advantages. For instance, microfluidic technology can be seamlessly integrated into textiles and wearable devices to achieve conformal thermal regulation on the skin. However, current challenges, such as slow temperature response, insufficient regulation accuracy, and limited regional temperature resolution, still need to be addressed. Future research should prioritize the development of adaptive temperature regulation systems that integrate high-throughput temperature sensing modules and control modules to achieve closed-loop precision temperature adjustment. Innovation in fluid-driving components represents another critical direction, with a focus on electroosmotic, passive capillary-driven pump-free systems, as well as piezoelectric micropumps. For wearable thermal management devices, sweat management cannot be overlooked. Comprehensive studies are expected to quantify sweat's effects on the microfluidics-based thermal regulation system. The development of hybrid thermal management systems that combine sweat-evaporative cooling mechanisms with microfluidic heat transfer capabilities enables enhanced temperature regulation for wearable devices. In biomedical applications, microfluidic thermal management systems hold particular promise due to their exceptional skin-conforming properties. They could be utilized for early trauma intervention, effectively mitigating pain, controlling bleeding, and reducing swelling. Furthermore, such systems could enhance wound care by maintaining an optimal thermal environment to promote faster healing. Future developments should focus on creating

intelligent systems that combine real-time physiological monitoring with adaptive thermal control, potentially revolutionizing personalized medical therapies and preventive care.

## 6. Conclusion

In this review, we systematically examine the recent advances in microfluidics-based thermal management devices for flexible electronics, focusing on solutions that address the increasing thermal load in highly integrated multifunctional platforms. The core goal of these innovations lies in maintaining optimal operating temperature and excellent thermal comfort when integrated on flexible substrates. Microfluidics-based thermoregulation systems primarily utilize the high specific surface area of microchannels, which are designed to conform to heat source geometries. As the fluid medium circulates through these microchannels, it efficiently absorbs and transports heat away from the electric components. Microfluidic devices offer the advantages of superior cooling capacity, easy integration, and high safety. Particularly noteworthy is the inherent flexibility and stretchability of these systems, which enables direct integration with high-power electronic components while maintaining efficient cooling performance. Our analysis focuses on two different types of cooling mechanisms, the single-phase cooling mechanism and flow boiling cooling mechanism. Subsequently, we critically evaluate fluid media, providing comprehensive comparisons of PCMs, liquid metals, and aqueous solutions in terms of their thermal properties and practical limitations. Channel geometry is also a critical factor in determining heat dissipation performance, primarily influencing heat transfer efficiency through factors such as the fluid flow path and contact time. Herein, we briefly discussed the microchannel configurations, *e.g.*, serpentine channels, spiral, and bio-inspired flow channels. Microfluidics-based thermal management systems have demonstrated unique advantages in diverse applications, including thermal haptic feedback, integrated circuits, smart thermoregulatory textiles, and biomedical applications. In these scenarios, conventional active and passive cooling approaches often suffer from fundamental limitations such as insufficient response time and inadequate cooling performance, or encounter difficulties in achieving miniaturization and flexibility requirements.

In conclusion, microfluidics-based thermal management has emerged as a potentially transformative technology, demonstrating excellent integration with flexible electronics. This field is witnessing rapid innovation in hybrid cooling solutions designed to address severe thermal challenges posed by next-generation, high-power integrated electronics. Driven by breakthroughs in advanced manufacturing and novel materials, microfluidic thermal management systems evolve from experimental prototypes to commercial components. This transition demonstrates their irreplaceable role in ensuring device safety, optimizing thermal

performance, and guaranteeing long-term reliability in electronic platforms.

## Conflicts of interest

There are no conflicts to declare.

## Data availability

No new data was generated or analyzed in this study. All data discussed are from previously published sources cited in the manuscript.

## Acknowledgements

This work was supported by City University of Hong Kong (grant no. 9667221, 9678274 and 9610444), as part of the InnoHK Project 2.2-AI-based 3D ultrasound imaging algorithm at Hong Kong Centre for Cerebro-cardiovascular Health Engineering (COCHE), and the Research Grants Council of the Hong Kong Special Administrative Region (grants no. RFS2324-1S03, 11213721, 11215722, 11211523).

## References

- 1 E. Song, J. Li, S. M. Won, W. Bai and J. A. Rogers, *Nat. Mater.*, 2020, **19**, 590–603.
- 2 Y. Zhang, E. Rytkin, L. Zeng, J. U. Kim, L. Tang, H. Zhang, A. Mikhailov, K. Zhao, Y. Wang, L. Ding, X. Lu, A. Lantsova, E. Aprea, G. Jiang, S. Li, S. G. Seo, T. Wang, J. Wang, J. Liu, J. Gu, F. Liu, K. Bailey, Y. F. L. Li, A. Burrell, A. Pfenniger, A. Ardashev, T. Yang, N. Liu, Z. Lv, N. S. Purwanto, Y. Ying, Y. Lu, C. Hoepfner, A. Melisova, J. Gong, J. Jeong, J. Choi, A. Hou, R. Nolander, W. Bai, S. H. Jin, Z. Ma, J. M. Torkelson, Y. Huang, W. Ouyang, R. K. Arora, I. R. Efimov and J. A. Rogers, *Nature*, 2025, **640**, 77–86.
- 3 J. Li, H. Jia, J. Zhou, X. Huang, L. Xu, S. Jia, Z. Gao, K. Yao, D. Li, B. Zhang, Y. Liu, Y. Huang, Y. Hu, G. Zhao, Z. Xu, J. Li, C. K. Yiu, Y. Gao, M. Wu, Y. Jiao, Q. Zhang, X. Tai, R. H. Chan, Y. Zhang, X. Ma and X. Yu, *Nat. Commun.*, 2023, **14**, 5009.
- 4 B. Zhang, J. Li, J. Zhou, L. Chow, G. Zhao, Y. Huang, Z. Ma, Q. Zhang, Y. Yang, C. K. Yiu, J. Li, F. Chun, X. Huang, Y. Gao, P. Wu, S. Jia, H. Li, D. Li, Y. Liu, K. Yao, R. Shi, Z. Chen, B. L. Khoo, W. Yang, F. Wang, Z. Zheng, Z. Wang and X. Yu, *Nature*, 2024, **628**, 84–92.
- 5 X. Yu, H. Wang, X. Ning, R. Sun, H. Albadawi, M. Salomao, A. C. Silva, Y. Yu, L. Tian, A. Koh, C. M. Lee, A. Chempakasseril, P. Tian, M. Pharr, J. Yuan, Y. Huang, R. Oklu and J. A. Rogers, *Nat. Biomed. Eng.*, 2018, **2**, 165–172.
- 6 W. Heng, S. Solomon and W. Gao, *Adv. Mater.*, 2022, **34**, 2107902.
- 7 K. Yao, J. Zhou, Q. Huang, M. Wu, C. K. Yiu, J. Li, X. Huang, D. Li, J. Su, S. Hou, Y. Liu, Y. Huang, Z. Tian, J. Li, H. Li, R. Shi, B. Zhang, J. Zhu, T. H. Wong, H. Jia, Z. Gao, Y. Gao, Y. Zhou, W. Park, E. Song, M. Han, H. Zhang, J. Yu, L. Wang, W. J. Li and X. Yu, *Nat. Mach. Intell.*, 2022, **4**, 893–903.

- 8 H. Zhao, Y. Kim, H. Wang, X. Ning, C. Xu, J. Suh, M. Han, G. J. Pagan-Diaz, W. Lu, H. Li, W. Bai, O. Aydin, Y. Park, J. Wang, Y. Yao, Y. He, M. T. A. Saif, Y. Huang, R. Bashir and J. A. Rogers, *Proc. Natl. Acad. Sci. U. S. A.*, 2021, **118**, e2100077118.
- 9 M. Kang, H. Jeong, S.-W. Park, J. Hong, H. Lee, Y. Chae, S. Yang and J.-H. Ahn, *Sci. Adv.*, 2022, **8**, eabm6693.
- 10 X. Yu, Z. Xie, Y. Yu, J. Lee, A. Vazquez-Guardado, H. Luan, J. Ruban, X. Ning, A. Akhtar, D. Li, B. Ji, Y. Liu, R. Sun, J. Cao, Q. Huo, Y. Zhong, C. Lee, S. Kim, P. Gutruf, C. Zhang, Y. Xue, Q. Guo, A. Chempakasseril, P. Tian, W. Lu, J. Jeong, Y. Yu, J. Cornman, C. Tan, B. Kim, K. Lee, X. Feng, Y. Huang and J. A. Rogers, *Nature*, 2019, **575**, 473–479.
- 11 Y. Huang, K. Yao, Q. Zhang, X. Huang, Z. Chen, Y. Zhou and X. Yu, *Chem. Soc. Rev.*, 2024, **53**, 8632–8712.
- 12 S. Patel, Z. Rao, M. Yang and C. Yu, *Adv. Funct. Mater.*, 2025, **35**, 2417906.
- 13 M. T. Flavin, K. H. Ha, Z. Guo, S. Li, J. T. Kim, T. Saxena, D. Simatos, F. Al-Najjar, Y. Mao, S. Bandapalli, C. Fan, D. Bai, Z. Zhang, Y. Zhang, E. Flavin, K. E. Madsen, Y. Huang, L. Emu, J. Zhao, J. Y. Yoo, M. Park, J. Shin, A. G. Huang, H. S. Shin, J. E. Colgate, Y. Huang, Z. Xie, H. Jiang and J. A. Rogers, *Nature*, 2024, **635**, 345–352.
- 14 Y. Kou, K. Sun, J. Luo, F. Zhou, H. Huang, Z.-S. Wu and Q. Shi, *Energy Storage Mater.*, 2021, **34**, 508–514.
- 15 S. Lee, S. H. Byun, C. Y. Kim, S. Cho, S. Park, J. Y. Sim and J. W. Jeong, *Adv. Mater.*, 2022, **34**, e2204805.
- 16 Y. Zhou, Z.-Y. Dong, W.-P. Hsieh, A. F. Goncharov and X.-J. Chen, *Nat. Rev. Phys.*, 2022, **4**, 319–335.
- 17 S. Jiang and G. Hong, *Science*, 2022, **377**, 28–29.
- 18 R. van Erp, R. Soleimanzadeh, L. Nela, G. Kampitsis and E. Matioli, *Nature*, 2020, **585**, 211–216.
- 19 T. Wei, *Nature*, 2020, **585**, 188–189.
- 20 Y. Meng, Z. Zhang, H. Wu, R. Wu, J. Wu, H. Wang and Q. Pei, *Nat. Energy*, 2020, **5**, 996–1002.
- 21 T. Sun, B. Feng, J. Huo, Y. Xiao, W. Wang, J. Peng, Z. Li, C. Du, W. Wang, G. Zou and L. Liu, *Nano-Micro Lett.*, 2023, **16**, 14.
- 22 S. Dai, Y. Dai, Z. Zhao, F. Xia, Y. Li, Y. Liu, P. Cheng, J. Strzalka, S. Li, N. Li, Q. Su, S. Wai, W. Liu, C. Zhang, R. Zhao, J. J. Yang, R. Stevens, J. Xu, J. Huang and S. Wang, *Matter*, 2022, **5**, 3375–3390.
- 23 B. Ramakrishnan, H. Alissa, I. Manousakis, R. Lankston, R. Bianchini, W. Kim, R. Baca, P. A. Misra, I. Goiri, M. Jalili, A. Raniwala, B. Warriar, M. Monroe, C. Belady, M. Shaw and M. Fontoura, *IEEE Trans. Compon., Packag., Manuf. Technol.*, 2021, **11**, 1703–1715.
- 24 Z. Zhang, X. Wang and Y. Yan, *e-Prime - Adv. Electr. Eng. Electron. Energy*, 2021, **1**, 100009.
- 25 Y. Fang, G. Chen, M. Bick and J. Chen, *Chem. Soc. Rev.*, 2021, **50**, 9357–9374.
- 26 G. Lv and J. Zhu, *Adv. Funct. Mater.*, 2025, **35**, 202420708.
- 27 Y. Xu, D. Kraemer, B. Song, Z. Jiang, J. Zhou, J. Loomis, J. Wang, M. Li, H. Ghasemi, X. Huang, X. Li and G. Chen, *Nat. Commun.*, 2019, **10**, 1771.
- 28 D. H. Ho, C. Hu, L. Li and M. D. Bartlett, *Nat. Electron.*, 2024, **7**, 1015–1024.
- 29 T. Pan, M. Pharr, Y. Ma, R. Ning, Z. Yan, R. Xu, X. Feng, Y. Huang and J. A. Rogers, *Adv. Funct. Mater.*, 2017, **27**, 1702589.
- 30 Z. Wang, Z. Wu, L. Weng, S. Ge, D. Jiang, M. Huang, D. M. Mulvihill, Q. Chen, Z. Guo, A. Jazzar, X. He, X. Zhang and B. B. Xu, *Adv. Funct. Mater.*, 2023, **33**, 2301549.
- 31 Y. Peng and Y. Cui, *Joule*, 2020, **4**, 724–742.
- 32 K. Lin, S. Chen, Y. Zeng, T. C. Ho, Y. Zhu, X. Wang, F. Liu, B. Huang, C. Y.-H. Chao, Z. Wang and C. Y. Tso, *Science*, 2023, **382**, 691–697.
- 33 M. H. Kang, G. J. Lee, J. H. Lee, M. S. Kim, Z. Yan, J. W. Jeong, K. I. Jang and Y. M. Song, *Adv. Sci.*, 2021, **8**, 2004885.
- 34 Y. Jung, M. Kim, S. Jeong, S. Hong and S. H. Ko, *ACS Nano*, 2024, **18**, 2312–2324.
- 35 J. Zhou, T. G. Chen, Y. Tsurimaki, A. Hajji-Ahmad, L. Fan, Y. Peng, R. Xu, Y. Wu, S. Assawaworrarit, S. Fan, M. R. Cutkosky and Y. Cui, *Joule*, 2023, **7**, 2830–2844.
- 36 J. Mao, G. Chen and Z. Ren, *Nat. Mater.*, 2020, **20**, 454–461.
- 37 R. Ma, Z. Zhang, K. Tong, D. Huber, R. Kornbluh, Y. S. Ju and Q. Pei, *Science*, 2017, **357**, 1130–1134.
- 38 J. Xiang, C. Zhang, Y. Gao, W. Schmidt, K. Schmalzl, C.-W. Wang, B. Li, N. Xi, X.-Y. Liu, H. Jin, G. Li, J. Shen, Z. Chen, Y. Qi, Y. Wan, W. Jin, W. Li, P. Sun and G. Su, *Nature*, 2024, **625**, 270–275.
- 39 M. B. Kulkarni and S. Goel, *Sens. Actuators, A*, 2022, **341**, 113590.
- 40 S. Apoorva, N.-T. Nguyen and K. R. Sreejith, *Lab Chip*, 2024, **24**, 1833–1866.
- 41 S. Mehraji and D. L. DeVoe, *Lab Chip*, 2024, **24**, 1154–1174.
- 42 T. L. Zhang, D. Di Carlo, C. T. Lim, T. Y. Zhou, G. Z. Tian, T. Tang, A. Q. Shen, W. H. Li, M. Li, Y. Yang, K. Goda, R. P. Yan, C. Lei, Y. Hosokawa and Y. Yalikun, *Biotechnol. Adv.*, 2024, **71**, 108317.
- 43 A. Jahanbakhshi, A. A. Nadooshan and M. Bayareh, *J. Energy Storage*, 2022, **49**, 104128.
- 44 J. Love Christopher, J. R. Anderson and G. M. Whitesides, *MRS Bull.*, 2001, **26**, 523–528.
- 45 Y. F. Li, J. X. Zhang, W. Han, B. H. Liu, M. J. Zhai, N. Li, Z. Y. Wang and J. Zhao, *Adv. Healthcare Mater.*, 2024, **13**, 202400981.
- 46 M. J. Xie, Z. X. Fu, C. F. Lu, S. F. Wu, L. Pan, Y. He, Y. Sun and J. Wang, *Bio-Des. Manuf.*, 2024, **7**, 611–623.
- 47 M. Hanze, A. Piper and M. M. Hamed, *Lab Chip*, 2024, **25**, 28–40.
- 48 J. Chen, Y. Shi, B. Ying, Y. Hu, Y. Gao, S. Luo and X. Liu, *Mater. Horiz.*, 2024, **11**, 2010–2020.
- 49 J. Li, Y. Fu, J. Zhou, K. Yao, X. Ma, S. Gao, Z. Wang, J.-G. Dai, D. Lei and X. Yu, *Sci. Adv.*, 2023, **9**, eadg1837.
- 50 X. Zhang, X. Chao, L. Lou, J. Fan, Q. Chen, B. Li, L. Ye and D. Shou, *Compos. Commun.*, 2021, **23**, 100595.
- 51 M. D. Bartlett, N. Kazem, M. J. Powell-Palm, X. Huang, W. Sun, J. A. Malen and C. Majidi, *Proc. Natl. Acad. Sci. U. S. A.*, 2017, **114**, 2143–2148.
- 52 Z. Li, H. Luo, Y. Jiang, H. Liu, L. Xu, K. Cao, H. Wu, P. Gao and H. Liu, *Appl. Therm. Eng.*, 2024, **251**, 123612.

- 53 T. Gao, Z. Yang, C. Chen, Y. Li, K. Fu, J. Dai, E. M. Hitz, H. Xie, B. Liu, J. Song, B. Yang and L. Hu, *ACS Nano*, 2017, **11**, 11513–11520.
- 54 X. Zhou, S. Xu, Z. Wang, L. Hao, Z. Shi, J. Zhao, Q. Zhang, K. Ishizaki, B. Wang and J. Yang, *Adv. Sci.*, 2022, **9**, 2103592.
- 55 S. Nie, M. Cai, H. Yang, L. Shen, S. Wang, Y. Zhu and J. Song, *npj Flexible Electron.*, 2022, **6**, 1.
- 56 N. Sun and X. Li, *J. Mater. Sci.*, 2021, **56**, 15937–15949.
- 57 R. A. Kishore, A. Nozariasbmarz, B. Poudel, M. Sanghadasa and S. Priya, *Nat. Commun.*, 2019, **10**, 1765.
- 58 Y. Huang, J. Zhou, P. Ke, X. Guo, C. K. Yiu, K. Yao, S. Cai, D. Li, Y. Zhou, J. Li, T. H. Wong, Y. Liu, L. Li, Y. Gao, X. Huang, H. Li, J. Li, B. Zhang, Z. Chen, H. Zheng, X. Yang, H. Gao, Z. Zhao, X. Guo, E. Song, H. Wu, Z. Wang, Z. Xie, K. Zhu and X. Yu, *Nat. Electron.*, 2023, **6**, 1245–1254.
- 59 Z. Wang, Y. Bo, P. Bai, S. Zhang, G. Li, X. Wan, Y. Liu, R. Ma and Y. Chen, *Science*, 2023, **382**, 1291–1296.
- 60 H. Wu, Y. Zhu, W. Yan, S. Zhang, W. Budiman, K. Liu, J. Wu, Y. Meng, X. Zhao, A. Mehta, S. Kaur and Q. Pei, *Science*, 2024, **386**, 546–551.
- 61 J. T. Reeder, Z. Xie, Q. Yang, M.-H. Seo, Y. Yan, Y. Deng, K. R. Jenkins, S. R. Krishnan, C. Liu, S. McKay, E. Patnaude, A. Johnson, Z. Zhao, M. J. Kim, Y. Xu, I. Huang, R. Avila, C. Felicelli, E. Ray, X. Guo, W. Z. Ray, Y. Huang, M. R. MacEwan and J. A. Rogers, *Science*, 2022, **377**, 109–115.
- 62 S. Yan, Q. Yuan, J. Wu and Z. Jia, *Front. Bioeng. Biotechnol.*, 2022, **10**, 1094294.
- 63 B. Zhao, *Sci. Rep.*, 2021, **11**, 16762.
- 64 J. D. Hardy and E. F. DuBois, *Proc. Natl. Acad. Sci. U. S. A.*, 1937, **23**, 624–631.
- 65 X. Zhao, T. Li, H. Xie, H. Liu, L. Wang, Y. Qu, S. C. Li, S. Liu, A. H. Brozena, Z. Yu, J. Srebric and L. Hu, *Science*, 2023, **382**, 684–691.
- 66 J. Liang, J. Wu, J. Guo, H. Li, X. Zhou, S. Liang, C.-W. Qiu and G. Tao, *Natl. Sci. Rev.*, 2023, **10**, nwac208.
- 67 Y. Wang, Y. Wang, T. He and N. Mao, *Renewable Energy*, 2024, **235**, 121273.
- 68 Y. Liu, X. Bu, R. Liu, M. Feng, Z. Zhang, M. He, J. Huang and Y. Zhou, *Chem. Eng. J.*, 2024, **481**, 148780.
- 69 H. Tang, C. Guo, F. Fan, H. Pan, Q. Xu and D. Zhao, *Energy Environ. Sci.*, 2024, **17**, 4498–4507.
- 70 C.-Q. Ma, C.-H. Xue, W. Fan, X.-J. Guo, J. Cheng, M.-C. Huang, H.-D. Wang, Y.-G. Wu, B.-Y. Liu and S.-Q. Lv, *ACS Sustainable Chem. Eng.*, 2024, **12**, 5695–5704.
- 71 Y. Zhang, X. Du, J. Huangfu, K. Chen, X. Han, C. Xiao and Q. Huang, *Chem. Eng. J.*, 2024, **490**, 151831.
- 72 Y. Zhang, J. Gao, S. Zhu, J. Li, H. Lai, Y. Peng and L. Miao, *ACS Appl. Mater. Interfaces*, 2022, **14**, 15317–15323.
- 73 S. Jia, H. Ma, S. Gao, L. Yang and Q. Sun, *Small*, 2024, **20**, 2405019.
- 74 L. Chow, G. Zhao, P. Wu, X. Huang, J. Li, J. Li, W. Wang, G. Guo, Z. Li, J. Wang, J. Zhou, Y. Yang, Y. Gao, B. Zhang, Q. Zhang, D. Li, Y. Huang, K. Yao, J. Lu and X. Yu, *Bio-Des. Manuf.*, 2024, **7**, 453–462.
- 75 S. Hong, Y. Gu, J. K. Seo, J. Wang, P. Liu, Y. S. Meng, S. Xu and R. Chen, *Sci. Adv.*, 2019, **5**, eaaw0536.
- 76 J. Li, A. Torelló, V. Kovacova, U. Prah, A. Aravindhnan, T. Granzow, T. Usui, S. Hirose and E. Defay, *Science*, 2023, **382**, 801–805.
- 77 Y. Wang, Z. Zhang, T. Usui, M. Benedict, S. Hirose, J. Lee, J. Kalb and D. Schwartz, *Science*, 2020, **370**, 129–133.
- 78 Y. Meng, J. Pu and Q. Pei, *Joule*, 2021, **5**, 780–793.
- 79 X. Qian, X. Chen, L. Zhu and Q. M. Zhang, *Science*, 2023, **380**, eadg0902.
- 80 K. Zou, P. Bai, K. Li, F. Luo, J. Liang, L. Lin, R. Ma, Q. Li, S. Jiang, Q. Wang and G. Zhang, *Nat. Commun.*, 2024, **15**, 6670.
- 81 H. Cui, Q. Zhang, Y. Bo, P. Bai, M. Wang, C. Zhang, X. Qian and R. Ma, *Joule*, 2022, **6**, 258–268.
- 82 J. Shi, D. Han, Z. Li, L. Yang, S.-G. Lu, Z. Zhong, J. Chen, Q. M. Zhang and X. Qian, *Joule*, 2019, **3**, 1200–1225.
- 83 D. Han, Y. Zhang, C. Huang, S. Zheng, D. Wu, Q. Li, F. Du, H. Duan, W. Chen, J. Shi, J. Chen, G. Liu, X. Chen and X. Qian, *Nature*, 2024, **629**, 1041–1046.
- 84 H. Chen, T. Zhang, Q. Gao, J. Lv, H. Chen and H. Huang, *Energy*, 2025, **316**, 134575.
- 85 H. Chen, Y. Zhang, L. Huang, X. Zhao, X. Ma, Z. Ma, J. Hou, J. Wei, P. Di Marco, O. Mahian and N. Hao, *Chem. Eng. J.*, 2023, **465**, 142799.
- 86 X. W. Zhang, H. Zhang, D. T. Li, H. Xu, Y. Huang, Y. Liu, D. M. Wu and J. Y. Sun, *Composites, Part B*, 2021, **224**, 109207.
- 87 P. Vishwakarma, S. N. Maurya, W. J. Luo and B. Panigrahi, *J. Micromech. Microeng.*, 2025, **35**, 065004.
- 88 W.-J. Luo, P. Vishwakarma, C.-C. Hsieh and B. Panigrahi, *Appl. Therm. Eng.*, 2022, **216**, 119142.
- 89 M. K. He, X. Zhong, X. H. Lu, J. W. Hu, K. P. Ruan, H. Guo, Y. L. Zhang, Y. Q. Guo and J. W. Gu, *Adv. Mater.*, 2024, **36**, 2410186.
- 90 R. Tarcan, M. Handrea-Dragan, C. I. Leordean, R. C. Cioban, G. Z. Kiss, D. Zaharie-Butucel, C. Farcau, A. Vulpoi, S. Simon and I. Botiz, *J. Appl. Polym. Sci.*, 2022, **139**, e53238.
- 91 Y. Bai, S. T. Zhou, X. Lei, H. W. Zou and M. Liang, *J. Appl. Polym. Sci.*, 2022, **139**, e52895.
- 92 L. L. Wu, Y. Z. Wang, Y. F. Gao, Y. R. Zhang, L. Zhou, J. Li and J. M. Zhang, *Polym. Compos.*, 2024, **45**, 12857–12869.
- 93 Z. Han and A. Fina, *Prog. Polym. Sci.*, 2011, **36**, 914–944.
- 94 A. A. Balandin, S. Ghosh, W. Z. Bao, I. Calizo, D. Teweldebrhan, F. Miao and C. N. Lau, *Nano Lett.*, 2008, **8**, 902–907.
- 95 K. Hirao, K. Watari, H. Hayashi and M. Kitayama, *MRS Bull.*, 2001, **26**, 451–455.
- 96 S. I. Kim, J. Y. Moon, S. K. Hyeong, S. Ghods, J. S. Kim, J. H. Choi, D. S. Park, S. Bae, S. H. Cho, S. K. Lee and J. H. Lee, *Nat. Commun.*, 2024, **15**, 2172.
- 97 S. D. Zhang, X. Li, Y. X. Sun, J. B. Zeng, S. L. Zhu, W. Q. Song, Y. Zhou, X. F. Ren, C. X. Hai and Y. Shen, *Sol. Energy Mater. Sol. Cells*, 2022, **238**, 111620.
- 98 Z. J. He, H. T. Ma and S. L. Lu, *J. Energy Storage*, 2024, **90**, 111906.
- 99 J. Thakkar, N. Bowen, A. C. Chang, P. Horwath, M. J. Sobkowicz and J. Kosny, *Buildings*, 2022, **12**, 1762.

- 100 P. Zhang, X. Xiao and Z. W. Ma, *Appl. Energy*, 2016, **165**, 472–510.
- 101 D. Y. Zhou, Y. H. Zhou, J. W. Yuan and Y. C. Liu, *J. Nanomater.*, 2020, **2020**, 1648080.
- 102 K. Y. Yu, M. J. Jia, W. C. Tian, Y. Z. Yang and Y. S. Liu, *Energy*, 2024, **290**, 130301.
- 103 L. X. Luo, W. X. Luo, W. J. Chen, X. W. Hu, Y. Ma, S. K. Xiao, Q. L. Li and X. X. Jiang, *Sol. Energy*, 2023, **255**, 146–156.
- 104 N. Acharya, F. Mabood and I. A. Badruddin, *Int. Commun. Heat Mass Transfer*, 2022, **134**, 106019.
- 105 L. Huang, J. Hou, L. Ma, Z. Ding, Y. Yu, J. Wu, X. Yu, W. Zhou, Z. Chen and N. Hao, *ACS Appl. Mater. Interfaces*, 2025, **17**, 23277–23285.
- 106 X. Zhao, L. Huang, J. S. Hou, Z. H. Ding, L. Ma, J. J. Wu, D. Y. Li, Y. L. Yao, Z. Z. Chen and N. J. Hao, *Chem. Eng. J.*, 2025, **503**, 158227.
- 107 E. Farsad, S. P. Abbasi, M. S. Zabihi and J. Sabbaghzadeh, *Heat Mass Transfer*, 2011, **47**, 479–490.
- 108 X. Y. Tang, Q. Xu, H. Y. Yu, C. Y. Pei and L. J. Guo, *Appl. Therm. Eng.*, 2025, **261**, 125077.
- 109 H. Waqas, S. A. Khan, U. Farooq, T. Muhammad, A. Alshehri and S. Yasmin, *Sci. Rep.*, 2022, **12**, 8035.
- 110 Y. Deng, M. Zhang, Y. Jiang and J. Liu, *Energy Convers. Manage.*, 2022, **259**, 115591.
- 111 C. Chande, N. Riaz, V. Harbour, H. Noor, M. Torralba, Y. H. Cheng, L. Zhenglong, A. Tong, R. Voronov and S. Basuray, *Technology*, 2021, **8**, 50–57.
- 112 D. H. Han, U. Oh and J.-K. Park, *ACS Omega*, 2023, **8**, 19128–19136.
- 113 R. Ito, Y. Takata, Y. Tanaka, H. Toshiyoshi and T. Suzuki, *Mater. Des.*, 2025, **252**, 113805.
- 114 V. H. Cabrera-Moreta, J. Casals-Terré and E. Salguero, *Processes*, 2024, **12**, 1066.
- 115 L. Pezzana, G. Riccucci, S. Spriano, D. Battezzore, M. Sangermano and A. Chiappone, *Nanomaterials*, 2021, **11**, 373.
- 116 H. Tan, L. W. Wu, M. Y. Wang, Z. H. Yang and P. G. Du, *Int. J. Heat Mass Transfer*, 2019, **129**, 681–689.
- 117 P. Trogadas, J. I. S. Cho, T. P. Neville, J. Marquis, B. Wu, D. J. L. Brett and M. O. Coppens, *Energy Environ. Sci.*, 2018, **11**, 136–143.
- 118 H. Li, X. H. Ding, F. Z. Meng, D. L. Jing and M. Xiong, *Int. J. Heat Mass Transfer*, 2019, **144**, 118638.
- 119 A. F. Al-Neama, N. Kapur, J. Summers and H. M. Thompson, *Appl. Therm. Eng.*, 2017, **116**, 709–723.
- 120 H. M. Jaffal, N. S. Mahmoud, A. A. Imran and A. Hasan, *Int. J. Therm. Sci.*, 2023, **184**, 107955.
- 121 M. Gorzin, A. A. Ranjbar and M. J. Hosseini, *Energy Rep.*, 2022, **8**, 3375–3385.
- 122 B. Cao and Z. Wu, *Int. J. Heat Mass Transfer*, 2025, **236**, 126411.
- 123 W. Raza, D. Ansari, J. H. Jeong, A. Samad and C. Duwig, *Appl. Therm. Eng.*, 2024, **241**, 122454.
- 124 F. Alnaimat, A. Rahhal and B. Mathew, *Results Eng.*, 2024, **21**, 101896.
- 125 Y. Alihosseini, Y. Oghabneshin, A. R. Bari, S. Moslemi, M. Zabetian Targhi, W. Guo and A. Mashhadian, *Case Stud. Therm. Eng.*, 2024, **53**, 103888.
- 126 P. Xu, J. Zhu, L. Xu, X. Zhang, S. Qiu, H. Gu and A. S. Mujumdar, *Int. J. Hydrogen Energy*, 2024, **93**, 328–337.
- 127 J. Yun, *Soft Sci.*, 2023, **3**, 12.
- 128 T. Zhong, H. Yi, J. Gou, J. Li, M. Liu, X. Gao, S. Chen, H. Guan, S. Liang, Q. He, R. Lin, Z. Long, Y. Wang, C. Shi, Y. Zhan, Y. Zhang, L. Xing, J. Zhong and X. Xue, *Nat. Commun.*, 2024, **15**, 1766.
- 129 D. B. Tuckerman and R. F. W. Pease, *IEEE Electron Device Lett.*, 1981, **2**, 126–129.
- 130 S. Mukherjee and I. Mudawar, *J. Electron. Packag.*, 2003, **125**, 431–441.
- 131 C. Krishnendu, P. Philip and P. Vamsee, *Adaptive Cooling of Integrated Circuits Using Digital Microfluidics*, Artech, 2007.
- 132 T. Dinh, H.-P. Phan, N. Kashaninejad, T.-K. Nguyen, D. V. Dao and N.-T. Nguyen, *Adv. Mater. Interfaces*, 2018, **5**, 1800764.
- 133 J. Ditre, R. R. Pearson, R. Cadotte, J. W. Hahn, D. Fetterolf, M. McNulty and D. Luppia, *IEEE Trans. Semicond. Manuf.*, 2016, **29**, 376–383.
- 134 Z. Wan, W. Yueh, Y. Joshi and S. Mukhopadhyay, *20th International Workshop on Thermal Investigations of ICs and Systems*, 2014, pp. 1–5.
- 135 Z. Liu, S. Qin, X. Chen, D. Chen and F. Wang, *Micromachines*, 2018, **9**, 165.
- 136 X. Du, Y. Ye, B. Jiao, Y. Kong, L. Yu, R. Liu, S. Yun, D. Lu, J. Qiao, Z. Liu and R. Yang, *Device*, 2025, **3**, 100576.
- 137 K.-Q. Ma and J. Liu, *J. Phys. D: Appl. Phys.*, 2007, **40**, 4722.
- 138 C. S. Sharma, S. Zimmermann, M. K. Tiwari, B. Michel and D. Poulikakos, *Int. J. Heat Mass Transfer*, 2012, **55**, 1957–1969.
- 139 S. C. Mohapatra and D. Loikits, *21st Annual IEEE Symposium on Semiconductor Thermal Measurement and Management (STHERM)*, 2005, pp. 354–360.
- 140 R. Yang, Z. Deng, B. Li and Y. Chen, *J. Appl. Phys.*, 2024, **135**, 21.
- 141 M. Smith, V. Cacucciolo and H. Shea, *Science*, 2023, **379**, 1327–1332.
- 142 J. Li, Y. Zhou, C. Jiang, D. Lei and X. Yu, *J. Mater. Chem. C*, 2024, **12**, 12179–12206.
- 143 Q. Zhang, H. Cheng, S. Zhang, Y. Li, Z. Li, J. Ma and X. Liu, *Chem. Eng. J.*, 2024, **488**, 151040.
- 144 Y. Peng, W. Li, B. Liu, W. Jin, J. Schaadt, J. Tang, G. Zhou, G. Wang, J. Zhou, C. Zhang, Y. Zhu, W. Huang, T. Wu, K. E. Goodson, C. Dames, R. Prasher, S. Fan and Y. Cui, *Nat. Commun.*, 2021, **12**, 6122.
- 145 A. Libanori, G. Chen, X. Zhao, Y. Zhou and J. Chen, *Nat. Electron.*, 2022, **5**, 142–156.
- 146 L. Chow, Q. Zhang, X. Huang, J. Zhang, J. Zhou, B. Zhu, J. Li, Y. Huang, B. Zhang, J. Li, P. Wu, Y. Gao, Z. Gao, G. Zhao, K. Yao, Y. Liu, J. Yip, Z. Yang and X. Yu, *Adv. Mater.*, 2024, **37**, 2406798.
- 147 T. Zhang, A. M. Ratajczak, H. Chen, J. A. Terrell and C. Chen, *ACS Sens.*, 2022, **7**, 3857–3866.

- 148 W. Gao, F. Liu, C. Yu, Y. Chen and X. Liu, *Renewable Sustainable Energy Rev.*, 2023, **171**, 112998.
- 149 G.-Q. Wen, R. Xie, W.-G. Liang, X.-H. He, W. Wang, X.-J. Ju and L.-Y. Chu, *Appl. Therm. Eng.*, 2015, **87**, 471–480.
- 150 X. Hu, M. Tian, T. Xu, X. Sun, B. Sun, C. Sun, X. Liu, X. Zhang and L. Qu, *ACS Nano*, 2020, **14**, 559–567.
- 151 Y. Jung, M. Kim, T. Kim, J. Ahn, J. Lee and S. H. Ko, *Nano-Micro Lett.*, 2023, **15**, 160.
- 152 P. Kotagama, A. Phadnis, K. C. Manning and K. Rykaczewski, *Adv. Mater. Technol.*, 2019, **4**, 1800690.
- 153 G.-X. Li, T. Dong, L. Zhu, T. Cui and S. Chen, *Chem. Eng. J.*, 2023, **453**, 139763.
- 154 S. Lee, S. Jang and Y. Cha, *iScience*, 2024, **27**, 111303.
- 155 D. T. Goetz, D. K. Owusu-Antwi and H. Culbertson, *2020 IEEE Haptics Symposium (HAPTICS)*, 2020, pp. 643–649.
- 156 S. Cai, P. Ke, T. Narumi and K. Zhu, *2020 IEEE Conference on Virtual Reality and 3D User Interfaces (VR)*, 2020, pp. 248–257.
- 157 Q. Zhuang, K. Yao, C. Zhang, X. Song, J. Zhou, Y. Zhang, Q. Huang, Y. Zhou, X. Yu and Z. Zheng, *Nat. Electron.*, 2024, **7**, 598–609.
- 158 Y. Gao, B. Zhang, Y. Liu, K. Yao, X. Huang, J. Li, T. H. Wong, Y. Huang, J. Li, J. Zhou, M. Wu, H. Li, Z. Gao, W. Park, C. K. Yiu, H. Jia, R. Shi, D. Li and X. Yu, *Adv. Mater. Technol.*, 2022, **8**, 2200759.
- 159 D. Li, J. Zhou, K. Yao, S. Liu, J. He, J. Su, Q. a. Qu, Y. Gao, Z. Song, C. Yiu, C. Sha, Z. Sun, B. Zhang, J. Li, L. Huang, C. Xu, T. H. Wong, X. Huang, J. Li, R. Ye, L. Wei, Z. Zhang, X. Guo, Y. Dai, Z. Xie and X. Yu, *Sci. Adv.*, 2022, **8**, eade2450.
- 160 Y. Liu, C. Yiu, Z. Song, Y. Huang, K. Yao, T. Wong, J. Zhou, L. Zhao, X. Huang, S. K. Nejad, M. Wu, D. Li, J. He, X. Guo, J. Yu, X. Feng, Z. Xie and X. Yu, *Sci. Adv.*, 2022, **8**, eabl6700.
- 161 G. Park, H. Park, J. Seo, J. C. Yang, M. Kim, B. J. Lee and S. Park, *Nat. Commun.*, 2023, **14**, 3049.
- 162 K. Hu, Y. Zhou, S. K. Sitaraman and M. M. Tentzeris, *Sci. Rep.*, 2023, **13**, 12515.
- 163 Q. Zhang, C. Qi, X. Wang, B. Zhu, W. Li, X. Xiao, H. Fu, S. Hu, S. Zhu, W. Xu and J. Zhu, *Nat. Chem. Eng.*, 2024, **1**, 301–310.
- 164 J. Ding, J. Jiang, Y. Tian, B. Su, M. Zeng, C. Wu, D. Wei, J. Sun, H. Luo and H. Fan, *ACS Appl. Mater. Interfaces*, 2024, **16**, 67444–67457.
- 165 P. Barnoon and F. Bakhshandehfard, *Case Stud. Therm. Eng.*, 2021, **26**, 101105.
- 166 D. Bai, Z. Zhao, R. Avila, D. Xia, Y. Huang, J. A. Rogers and Z. Xie, *J. Mech. Phys. Solids*, 2024, **190**, 105741.
- 167 Y. Huang, H. Li, T. Hu, J. Li, C. K. Yiu, J. Zhou, J. Li, X. Huang, K. Yao, X. Qiu, Y. Zhou, D. Li, B. Zhang, R. Shi, Y. Liu, T. H. Wong, M. Wu, H. Jia, Z. Gao, Z. Zhang, J. He, M. Zheng, E. Song, L. Wang, C. Xu and X. Yu, *Nano Lett.*, 2022, **22**, 5944–5953.
- 168 Q. Zhang, G. Zhao, Z. Li, F. Guo, Y. Huang, G. Guo, J. Wang, J. Zhou, L. Chow, X. Huang, X. He, Y. Gao, Z. Gao, K. Yao, Y. Qiu, Z. Zhao, B. Zhang, Y. Yang, Y. Liu, Y. Hu, M. Wu, J. Li, P. Wu, G. Xu, P. He, Z. Yang and X. Yu, *Biosens. Bioelectron.*, 2024, **263**, 116597.
- 169 J. Kim, J. S. Lee, S. Noh, E. Seo, J. Lee, T. Kim, S.-W. Cho, G. Kim, S. S. Kim and J. Park, *Biosens. Bioelectron.*, 2025, **277**, 117257.
- 170 J. Huang, C. Fan, Y. Ma and G. Huang, *Clin. Cosmet. Invest. Dermatol.*, 2024, **17**, 1251–1258.
- 171 L. I. Anatychuk, N. V. Pasechnikova, V. O. Naumenko, O. S. Zadorozhnyi, S. L. Danyliuk, M. V. Havryliuk, V. A. Tiumentsev and R. R. Kobylanskyi, *Phys. Chem. Solid State*, 2020, **21**, 140–145.
- 172 Z. Liu, D. Sun, B. Jiang, L. Shen, P. Zhou, C. Gao, Z. Jin, X. Liu, L. Yang and S. Tan, *Appl. Therm. Eng.*, 2023, **234**, 121277.
- 173 R. Su, J. Wen, Q. Su, M. S. Wiederoder, S. J. Koester, J. R. Uzarski and M. C. McAlpine, *Sci. Adv.*, 2020, **6**, eabc9846.
- 174 R. Maiti, L.-C. Gerhardt, Z. S. Lee, R. A. Byers, D. Woods, J. A. Sanz-Herrera, S. E. Franklin, R. Lewis, S. J. Matcher and M. J. Carré, *J. Mech. Behav. Biomed. Mater.*, 2016, **62**, 556–569.
- 175 S. K. Tiwari, S. Bhat and K. K. Mahato, *Sci. Rep.*, 2020, **10**, 9215.
- 176 X. Kang, J. Ma, H. Cha, H. H. W. B. Hansen, X. Chen, H. T. Ta, F. Tian, N.-T. Nguyen, A. Klimenko, J. Zhang and D. Yuan, *ACS Appl. Mater. Interfaces*, 2024, **16**, 61765–61773.
- 177 R. Takahashi, H. Miyazako, A. Tanaka, Y. Ueno and M. Yamaguchi, *Lab Chip*, 2021, **21**, 1307–1317.
- 178 I. Ramos, M. Gonçalves, I. M. Gonçalves, V. Carvalho, E. Fernandes, R. Lima and D. Pinho, *J. Mol. Liq.*, 2025, **434**, 127978.
- 179 M. A. Andersen and J. Schouenborg, *Sci. Rep.*, 2023, **13**, 16090.